REVISED Manuscript (text UNmarked) Click here to view linked References

Convenient PET-tracer production via SuFEx ^{18}F-fluorination of nanomolar precursor amounts

Nils Walter[a], Jan Bertram[a], Birte Drewes[a], Victor Bahutski[a], Marco Timmer[b], Markus B. Schütz[c], Felicia Krämer[d], Felix Neumaier[a,d], Heike Endepols[a,d,e], Bernd Neumaier[a,d,f,*], Boris D. Zlatopolskiy[a,d,f]

[a] Forschungszentrum Jülich GmbH, Institute of Neuroscience and Medicine, Nuclear Chemistry (INM-5), Wilhelm-Johnen-Straße, 52425 Jülich, Germany; n.walter@fz-juelich.de (NW), jbertra1@smail.uni-koeln.de (JB), b.drewes@fz-juelich.de (BD), vbaguts@yahoo.com (VB), f.neumaier@fz-juelich.de (FN)

[b] University of Cologne, Faculty of Medicine and Cologne University Hospital, Center for Neurosurgery, Kerpener Straße 62, 50937 Cologne, Germany; marco.timmer@uk-koeln.de (MT)

[c] University of Cologne, Faculty of Medicine and Cologne University Hospital, Institute of Diagnostic and Interventional Radiology, Kerpener Straße 62, 50937 Cologne, Germany; markus.schuetz@uk-koeln.de (MBS)

[d] University of Cologne, Faculty of Medicine and Cologne University Hospital, Institute of Radiochemistry and Experimental Molecular Imaging, Kerpener Straße 62, 50937 Cologne, Germany; maximiliane-felicia.kraemer1@uk-koeln.de (FK), heike.endepols@uk-koeln.de (HE), boris.zlatopolskiy@uk-koeln.de (BDZ)

[e] University of Cologne, Faculty of Medicine and Cologne University Hospital, Department of Nuclear Medicine, Kerpener Straße 62, 50937 Cologne, Germany

[f] Max Planck Institute for Metabolism Research, Gleueler Straße 50, 50931 Cologne, Germany

* correspondence: b.neumaier@fz-juelich.de

ABSTRACT: Recently, a protocol for radiolabeling of aryl fluorosulfates ("SuFEx click radiolabeling") using ultrafast ^{18}F/^{19}F isotopic exchange has been reported. Although promising, the original procedure turned out to be rather inefficient. However, systematic optimization of the reaction parameters allowed for development of a robust method for SuFEx radiolabeling which obviates the need for azeotropic drying, base addition and HPLC purification. The developed protocol enabled efficient ^{18}F-fluorination of low nanomolar amounts of aryl fluorosulfates in highly diluted solution (micromolar concentrations). It was successfully used to prepare a series of 29 [^{18}F]fluorosulfurylated phenols – including modified ezetimibe, α-tocopherol and etoposide, the two tyrosine derivatives Boc-([^{18}F]FS)Tyr-OMe and H-([^{18}F]FS)Tyr-OMe, the FAP-specific ligand [^{18}F]FS-UAMC1110, and the DPA-714 analog [^{18}F]FS-DPA – in fair to excellent yields. Preliminary evaluation demonstrated sufficient *in vivo* stability of radiofluorinated electron rich or neutral {Boc-Tyr([^{18}F]FS)-OMe) and H-([^{18}F]FS)Tyr-OMe} aryl fluorosulfates. Furthermore, [^{18}F]FS-DPA was identified as a promising tracer for visualization of TSPO expression.

KEYWORDS: imaging agents, positron emission tomography (PET), radiochemistry, radiopharmaceuticals, SuFEx click chemistry

Abbreviations: ^{18}F – fluorine-18; [^{18}F]F$^-$ – [^{18}F]fluoride; [^{18}F]FET – O-(2-[^{18}F]fluoroethyl)tyrosine; ACA – anterior cerebral artery; ACh – acetylcholine; AY – activity yield; FAP – fibroblast activation protein; n.c.a. – no carrier added; PET – positron emission tomography; RCC – radiochemical conversion; SPE – solid phase extraction; SuFEx – sulfur (VI) fluoride exchange; TSPO – translocator protein 18 kDa

1. Introduction

Positron emission tomography (PET) is a non-invasive imaging technique that allows for *in vivo* visualization and quantification of biochemical processes at the molecular level, by applying probes labeled with β^+-emitting isotopes [1]. As such, PET imaging has become an indispensable part of clinical praxis that is widely used for various diagnostic and prognostic applications, especially in the fields of oncology and neurology [1,2]. Among the available PET radionuclides, fluorine-18 (^{18}F) remains the most popular one [3], which is mainly attributable to its convenient availability in no carrier added (n.c.a.) form as [^{18}F]fluoride ([^{18}F]F$^-$) in amounts of up to 500 GBq. Furthermore, ^{18}F possesses favorable decay properties, comprising a low kinetic energy of emitted positrons ($E_{\beta max}$=0.634 MeV) and a half-life (109.8 min) which is optimal for many applications [3]. Additional advantages of ^{18}F over other radionuclides include certain physicochemical properties of fluorine, such as a low steric bulk and the ability to form strong, oftentimes hydrolytically and metabolically stable, covalent bonds with carbon as well as with heteroatoms like sulfur, silicon, phosphorus and boron [4].

Recently, Zheng *et al*. applied sulfur (VI) fluoride exchange (SuFEx) click chemistry for the preparation of aryl [^{18}F]fluorosulfates via instant ^{18}F/^{19}F isotopic exchange [5]. The novel procedure was reported to afford most radiolabeled products in >90% radiochemical conversions (RCCs; analytical radiochemical yields determined by HPLC) at ambient temperature using 160–500 nmol precursor [5]. Being interested in the utilization of novel, highly efficient radiofluorination protocols for accelerated development of PET probes [6–10], we selected SuFEx ^{18}F-fluorination for the rapid preparation of novel radiolabeled candidate tracers. However, in our hands, ^{18}F-incorporation under literature conditions was significantly lower than originally reported. This encouraged us to identify the factors underlying this discrepancy and to develop an alternative approach for SuFEx radiofluorination. The latter was successfully applied for the preparation of several radiolabeled model compounds and PET tracers, including amino acid esters, a novel FAP-inhibitor and a TSPO ligand.

2. Results and discussion

Initially, we studied SuFEx radiofluorination of 4-methoxyphenyl fluorosulfate (**1**) as a model substrate using the published procedure. Accordingly, **1** (20–50 µg) in MeCN (500–1000 µL) was briefly treated at ambient temperature with aliquots (15–35 MBq, 100–500 µL) of azeotropically dried [^{18}F]KF/K_2CO_3/$K_{2.2.2}$ that had been redissolved in MeCN. However, only 53±1% (n = 3) of the ^{18}F-activity could be resolubilized, indicating that the procedure was associated with significant losses of radioactivity to the vessel walls. In a first attempt to circumvent this problem, a solution of the precursor was directly added to the vial containing the dried [^{18}F]KF/K_2CO_3/$K_{2.2.2}$ and the reaction time

was increased to 20 min. However, these modifications only led to a minor improvement of radioactivity resolubilization. Likewise, even if the reaction volume was increased to 10 mL (cf. SI of [5], p. S108), 40±8% (n = 4) of the [^{18}F]F$^-$ still remained adsorbed to the reactor walls. In addition, the radiolabeling outcome varied strongly from run to run, so that RCCs of 12–85% (54±25%, n = 8) and 32–60% (n = 2) were observed for aliquot and one-pot ^{18}F-fluorinations, respectively. Similar results were also obtained with 3-ethynylphenyl sulfurofluoridate (**2**) (see Supporting Information for further details). A possible explanation for the almost quantitative conversions apparently obtained by Zheng et al. could be the strongly acidic mobile phase (10–100% MeCN in 0.5% TFA) which was used for HPLC analyses of the radiofluorinated products on silica-based SunFire C_{18} columns [5]. Under these conditions, [^{18}F]HF formed at pH < 3 was previously reported to be strongly retained on the stationary phase [11]. In order to evaluate if this was the case, we analyzed the crude 4-methoxyphenyl [^{18}F]fluorosulfate ([^{18}F]**1**) on SunFire C_{18} columns as used in the seminal publication or on SpeedROD C_{18} columns usually applied in our lab, both under neutral and acidic conditions (**Fig. 1**). Surprisingly, SunFire C_{18} columns adsorbed unreacted [^{18}F]F$^-$ almost completely, both under acidic and neutral conditions (**Fig. 1 A**, **B**). In contrast, recovery of radioactivity from SpeedROD C_{18} columns under acidic and neutral conditions was consistently >95% (**Fig. 1 C**, **D**).

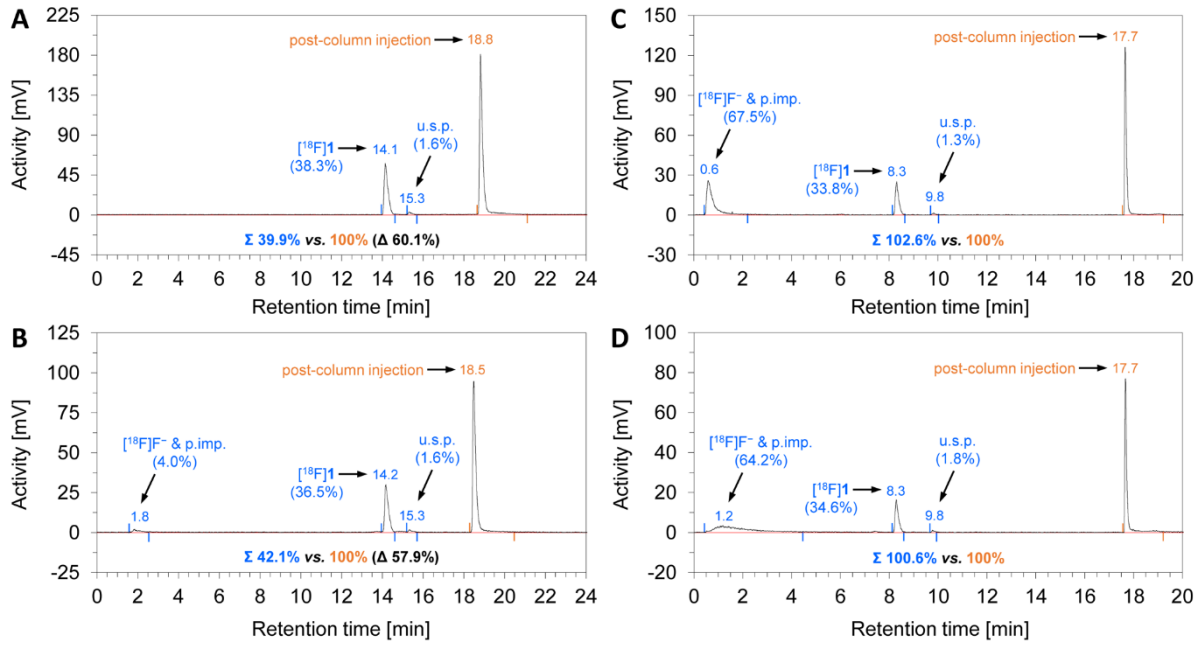

Figure 1. Radio-HPLC traces of crude [^{18}F]**1** obtained using: SunFire® C_{18} 100 Å, 3.5 µm, 4.6 × 150 mm (A and B) and Chromolith® SpeedROD RP-18e C_{18} 130 Å, 2 µm, 4.6 × 50 mm (C and D) columns. Conditions: injection loop: 20 µL, injection: 60 µL; **A**: eluent 0 min: 10% MeCN, 18 min: 100% MeCN, 18–25 min: 100% MeCN, flow rate: 1 mL/min; **B**: 0 min: 10% MeCN in 0.1% TFA, 18 min: 100% MeCN, 18–25 min: 100% MeCN, flow rate: 1 mL/min; **C** 0–2 min: 10% MeCN, 15 min: 90% MeCN, 15–20

min: 90% MeCN, flow rate: 2 mL/min; **D**: 0–2 min: 10% MeCN in 0.1% TFA, 15 min: 90% MeCN in 0.1% TFA, 15–20 min: 90% MeCN in 0.1% TFA, flow rate: 2 mL/min. Chromatograms are corrected for decay. The corresponding non-decay corrected chromatograms are provided in the Supporting Information (**SI**, **Fig. S1**). The post-column injection peak corresponds to the total radioactivity amount loaded onto the column. The difference between the decay-corrected integral of the post-column injection peak and the sum of the integrals of all decay-corrected peaks in the chromatogram provides an estimate of radioactivity (mainly $[^{18}F]F^-$) retained on the column. Abbreviations: p.imp – polar impurities (presumably $[^{18}F]HSO_3F$); u.s.p. – unknown side product.

In order to eliminate the solubility problem and avoid azeotropic drying, we tested the application of different organic salts for SuFEx radiolabeling (**Fig. 2**). To this end, $[^{18}F]F^-$ was loaded onto an anion exchange resin and eluted with a solution of the corresponding salt (10 µmol) in MeOH (1 mL) [12,13]. MeOH was removed at 80–90 °C within 3–7 min, and the residue was taken up in a solution of **1** (20 µg, 97 nmol) in MeCN (1 mL). The reaction mixture was then incubated without stirring at 40 °C for 5 min followed by addition of H_2O (0.5 mL). Under these conditions, the $[^{18}F]F^-$ elution efficacy was about 95% for all studied salts except DMAP·TfOH (**Fig. 2**). Me_4N salts enabled efficient $[^{18}F]F^-$ elution but were unsuitable for the subsequent radiolabeling reaction, presumably owing to their low solubility in MeCN. Application of the strongly basic salts Bu_4NOMe and Bu_4NOEt delivered highly irreproducible radiolabeling results, while incorporation yields of 60–85% and marginal (<5%) radioactivity adsorption on the reactor walls were observed for most other salts. In particular, radiolabeling reactions with the neutral salts Bu_4NClO_4 and $BnEt_3NCl$ afforded RCCs of about 85%. Among the latter, $BnEt_3NCl$, which cannot act as an oxidant like Bu_4NClO_4, afforded more reproducible ^{18}F-incorporation rates, and was therefore applied in most of the following experiments. Interestingly, using the neurotransmitter acetylcholine (ACh) as its chloride or iodide salt for $[^{18}F]F^-$ elution, $[^{18}F]$**1** could be produced in moderate RCCs of 33–35%.

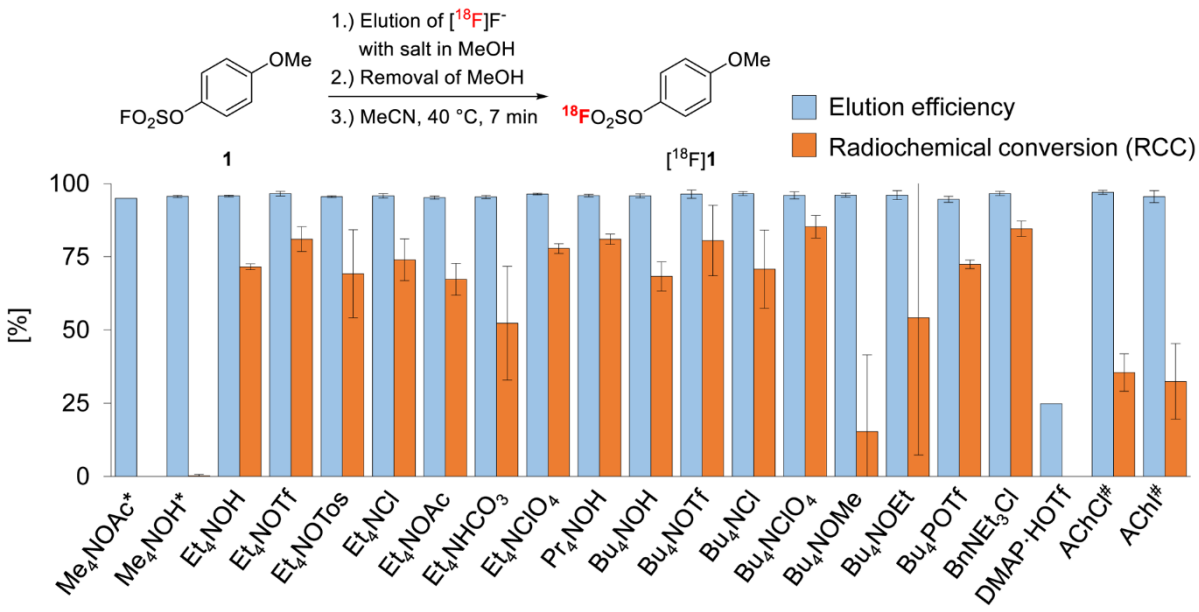

Figure 2. ^{18}F-Recovery and -incorporation using different salts: Bar graph shows the [^{18}F]F$^-$ elution efficacy (light blue bars) and radiochemical conversion (RCC, orange bars) for the reaction depicted above with the indicated salts. Conditions: Unless noted otherwise, [^{18}F]F$^-$ (10–30 MBq) was eluted from an anion exchange QMA cartridge with a solution of the corresponding salt (10 µmol) in MeOH (1 mL). MeOH was evaporated in a stream of Ar at 70–90 °C, the residue was taken up with a solution of **1** (20 µg, 97 nmol) in MeCN (1 mL) and the reaction mixture was heated at 40 °C for 7 min. Thereafter, H_2O (0.5 mL) was added to quench the reaction and solubilize surface-adsorbed [^{18}F]F$^-$ and the RCC was determined by radio-HPLC. Unless noted otherwise, all experiments were carried out at least in triplicate. * – experiments were carried out in duplicate; # – elution of [^{18}F]F$^-$ was carried out with 1.7 µmol (AChCl) or 1.5 µmol (AChI) of the corresponding salt in 0.7 mL MeOH. Abbreviations: ACh – acetylcholine.

Next, we evaluated the influence of solvent and reaction temperature on RCCs (**Fig. 3**). Whereas ^{18}F-incorporation rates in DMSO and propylene carbonate were only slightly lower than in MeCN (about 80%), radiolabeling in other solvents was less efficient (**Fig. 3A**). With regard to the reaction temperature, SuFEx ^{18}F/^{19}F isotopic exchange demonstrated a marked tolerance (**Fig. 3B**). At ambient temperature, [^{18}F]**1** was formed in RCCs of 74±0.4% after incubation for 3 min. At 40–70 °C, incorporation yields after 3 min amounted to >80%. When the reaction temperature was further increased, RCCs showed a gradual decrease (to 77±7% and 67±4% at 80 °C and 90 °C, respectively) indicating partial decomposition of the radiolabeled fluorosulfate [^{18}F]**1** at higher temperatures.

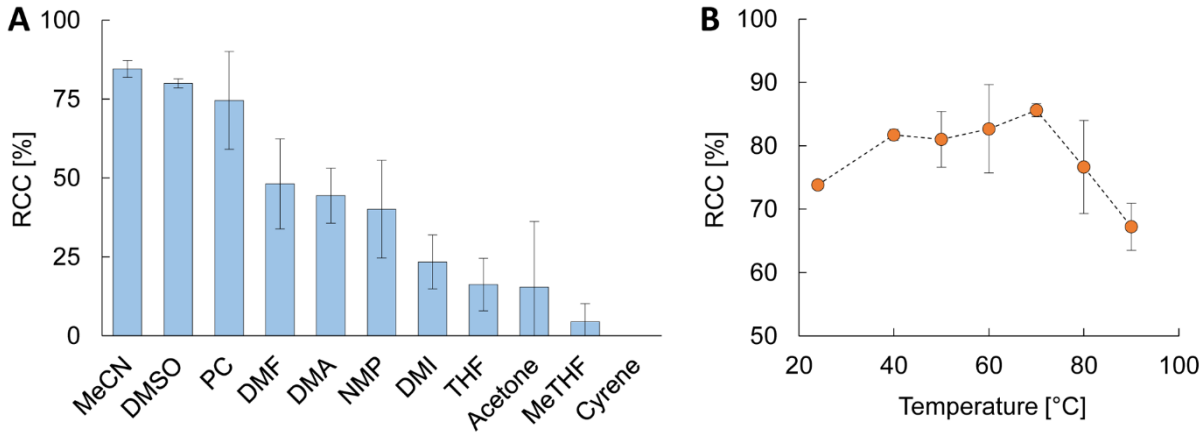

Figure 3. Dependence of radiochemical conversions (RCCs) on reaction solvent (**A**) and reaction temperature (**B**). Conditions: [^{18}F]F$^-$ (10–30 MBq) was eluted from an anion exchange QMA cartridge with a solution of $BnEt_3NCl$ (2.3 mg, 10 µmol) in MeOH (1 mL). MeOH was evaporated in a stream of Ar at 80–90 °C, the residue was taken up with a solution of **1** (20 µg, 97 nmol) in the appropriate solvent (A) or MeCN (B) (1 mL) and the reaction mixture was heated at 40 °C (A) or at the indicated temperatures (B) for 5 (A) or 3 (B) min. Thereafter, H_2O (0.5 mL) was added to quench the reaction and solubilize surface-adsorbed [^{18}F]F$^-$ and the RCC was determined by radio-HPLC. Experiments were carried out at least in duplicate. Abbreviations: DMA – dimethylacetamide; DMI – 1,3-dimethyl-2-imidazolidinone; DMF – dimethylformamide; DMSO – dimethyl sulfoxide; MeCN – acetonitrile; MeTHF – 2-methyltetrahydrofuran; NMP – *N*-methyl-2-pyrrolidone; PC – propylene carbonate.

Additionally, the radiolabeling kinetics were studied (**Fig. 4A**). At 40 °C, RCCs of >60% and >80% were already observed after 1 and 2 min, respectively, while a plateau of 85% was reached after 5 min.

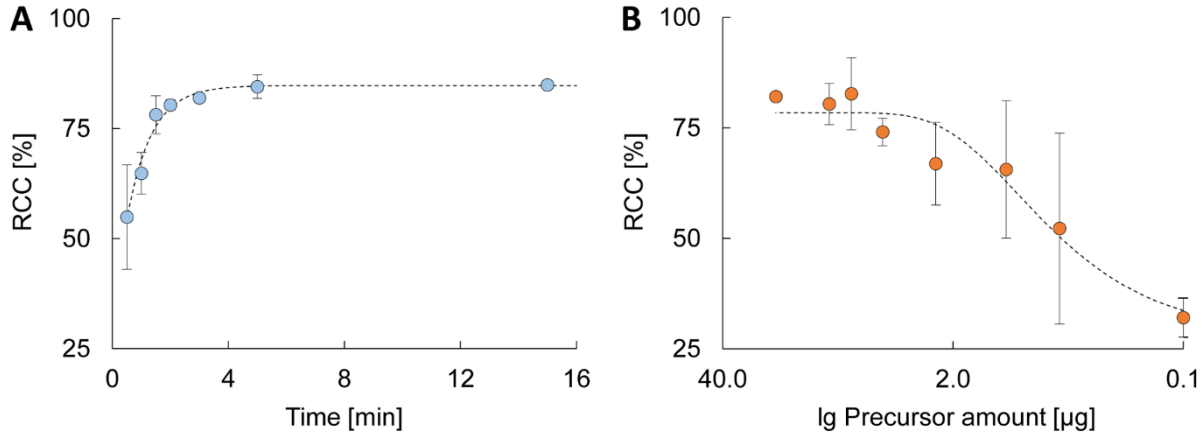

Figure 4. Kinetics and precursor amount dependence of radiolabeling. Shown is the dependence of radiochemical conversions (RCCs) on the reaction time (**A**) and amount of precursor (**B**). Note that B

was plotted with a base-10 logarithmic scale on the x-axis to facilitate visualization of the whole data range. Conditions: [^{18}F]F$^-$ (10−30 MBq) was eluted from an anion exchange QMA cartridge with a solution of $BnEt_3NCl$ (2.3 mg, 10 μmol) in MeOH (1 mL). MeOH was evaporated in a stream of Ar at 80–90 °C, the residue was taken up with a solution of **1** [20 μg, 97 nmol (A) or the indicated amounts (B)] in MeCN (1 mL) and the reaction mixture was heated at 40 °C for the indicated time periods (A) or for 5 min (B), respectively. Thereafter, H_2O (0.5 mL) was added to quench the reaction and solubilize surface-adsorbed [^{18}F]F$^-$ and the RCC was determined by radio-HPLC. Experiments were carried out at least in duplicate.

PET-tracers prepared via isotopic exchange are inevitably contaminated with comparably large amounts of the corresponding isotopically unmodified compound ("carrier") [14]. High carrier amounts can impair the image quality and may even lead to adverse pharmacological effects, impeding clinical application of the tracers. Consequently, the novel radiolabeling protocol was evaluated with respect to the influence of precursor amount on RCCs (**Fig. 5B**). Precursor loadings of ≥36 nmol (≥7.5 μg) reliably afforded [^{18}F]**1** in RCCs of 80% or more. Progressive reduction of the precursor amount from 36.4 to 4.9 nmol (from 7.5 to 1 μg) led to a gradual decrease of the incorporation yields to 66%. Impressively, even with precursor amounts as low as 2.4 or 0.5 nmol **1** (0.5 or 0.1 μg, respectively), ^{18}F-incorporation yields of 52% or 32%, respectively, were achieved, highlighting the extremely high efficacy of SuFEx radiolabeling.

To demonstrate the versatility of the procedure, we next radiofluorinated a series of structurally diverse model aryl fluorosulfates (**Fig. 5** and **6**). Moderately electron deficient, electron neutral and electron rich aryl fluorosulfates ([^{18}F]**2–17**) were prepared in RCCs of 65–93% at reaction temperatures of 23–40 °C. In the majority of cases, the optimal incubation time amounted to 3–5 min. Only for ^{18}F-labeled aldehyde [^{18}F]**6**, which was not completely stable under longer incubation times, the reaction time was reduced to 1 min. Highly electron deficient products, like [^{18}F]**19–21** and moderately electron deficient [^{18}F]**18** were markedly unstable under the selected reaction conditions. Thus, highest RCCs of up to 85% were in these cases obtained at 0 °C with incubation times of ≤30 s and 5 min, respectively. Noteworthy, 2-benzaldehyde derivative **19** was insufficiently stable even under such mild conditions, presumably owing to the destabilizing *ortho*-effect of the strongly electron-withdrawing carbonyl group, so that [^{18}F]**19** could at best be prepared in a moderate RCC of 48±2%. Nevertheless, after dilution of the reaction mixture with H_2O (1 mL), such radiolabeled compounds remained stable for at least 80 min. Likewise, after addition of 0.1 M NaH_2PO_4 or 0.1 M Na_2HPO_4 (1 mL), [^{18}F]**20** was not hydrolyzed for at least 70 min or 30 min, respectively. For the highly electron-rich carbazole derivative **22**, the highest ^{18}F-incorporation rate of 77±3% was obtained at 90 °C.

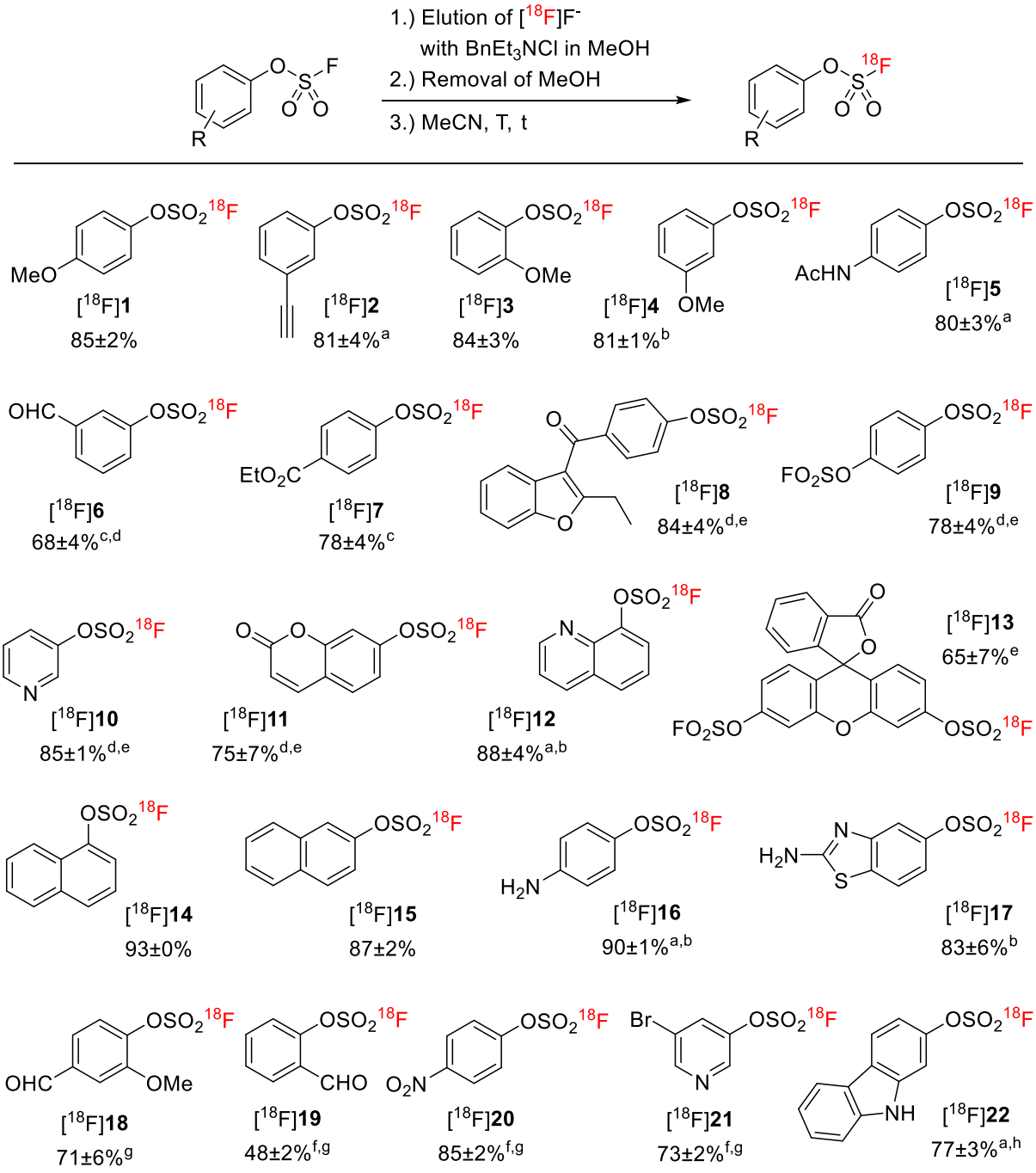

Figure 5. Substrate scope (model compounds) of the novel SuFEx radiolabeling protocol. Radiochemical conversions (RCCs) are indicated as mean±SD [%] (n=2–5). Conditions: precursor (20 µg), $BnEt_3NCl$ (0.4 mg), MeCN (1 mL), 40 °C, 5 min. [a] Reaction time: 3 min. [b] Reaction temperature: 60→40 °C. [c] Reaction time: 1 min. [d] Reaction temperature: 25 °C. [e] Reaction time: 2 min. [f] Reaction time: 0.5 min. [g] Reaction temperature: 0 °C. [h] Reaction temperature: 90 °C.

Using the optimized protocol, we also successfully prepared radiolabeled analogs of more complex compounds like ezetimibe, α-tocopherol and etoposide ([^{18}F]**23–25**, **Fig. 6**). Ezetimibe derivative **23**

was not completely stable under radiolabeling conditions, presumably due to opening of the sensitive β-lactam ring. In this case, a reduced incubation time of 2 min afforded [^{18}F]**23** in an RCC of 57±1% without noticeable formation of side products. For extremely electron-rich and sterically hindered fluorosulfates derived from α-tocopherol and etoposide, [^{18}F]**24** and [^{18}F]**25**, the highest ^{18}F-incorporation rates were observed at 105 °C and 4 min reaction time, amounting to 60±5% and 26±6%, respectively. Further increases of the reaction temperature and/or incubation time did not improve the RCCs but instead gave rise to formation of [^{18}F]FSO_3^- as a side product, indicating a limited stability of the respective aryl fluorosulfates at >100 °C.

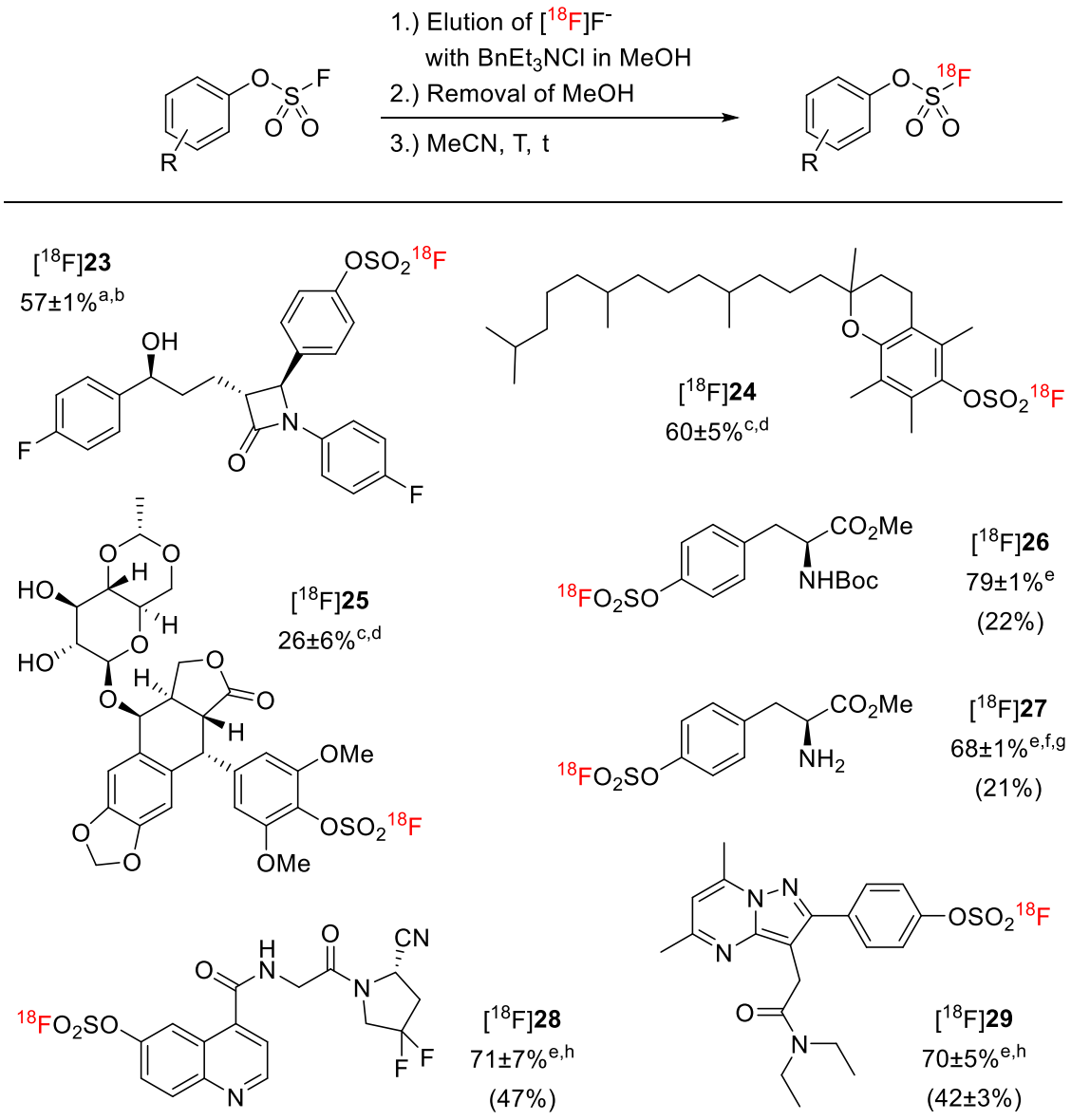

Figure 6. Substrate scope (analogs of natural compounds and pharmaceuticals as well as PET-tracers) of the novel SuFEx radiolabeling protocol. Radiochemical conversions (RCCs) are indicated as mean±SD [%] (n=2–5). Activity yields (AYs; non-decay corrected yield of analytically pure tracer) of SPE-purified and formulated radiolabeled compounds are shown in parentheses. Conditions: precur-

sor (20 µg), $BnEt_3NCl$ (0.4 mg), MeCN (1 mL), T, t. [a] Reaction temperature: 25 °C. [b] Reaction time: 2 min. [c] Reaction temperature: 105 °C. [d] Reaction time: 4 min. [e] Reaction temperature: 40 °C. [f] Reaction time: 7 min. [g] Et_4NOH was used instead of $BnEt_3NCl$. [h] Reaction time: 3 min.

In order to assess the metabolic stability of radiolabeled fluorosulfate-substituted aromatic amino acids, we produced Boc-Tyr([^{18}F]SO_2F)-OMe ([^{18}F]**26**) and subjected it to a preclinical evaluation in healthy mice (**Fig. 7**). [^{18}F]**26** was prepared by the standard protocol, isolated by solid phase extraction (SPE) and formulated as a ready-to-use solution with an activity yield (AY; non-decay corrected yield of analytically pure tracer) of 22% and a radiochemical purity of >98% within 50 min. The tracer demonstrated strong and sustained accumulation in liver (maximum SUV_{bw} 474±77, 0–30 min p.i.) and gastrointestinal tract (maximum SUV_{bw} 2043±935, 90–120 min p.i.), while bone radioactivity uptake was low (maximum SUV_{bw} 155±43, 90–120 min p.i.), indicating a high stability of [^{18}F]**26** against *in vivo* defluorination (**Fig. 7** and **Tab. 1**).

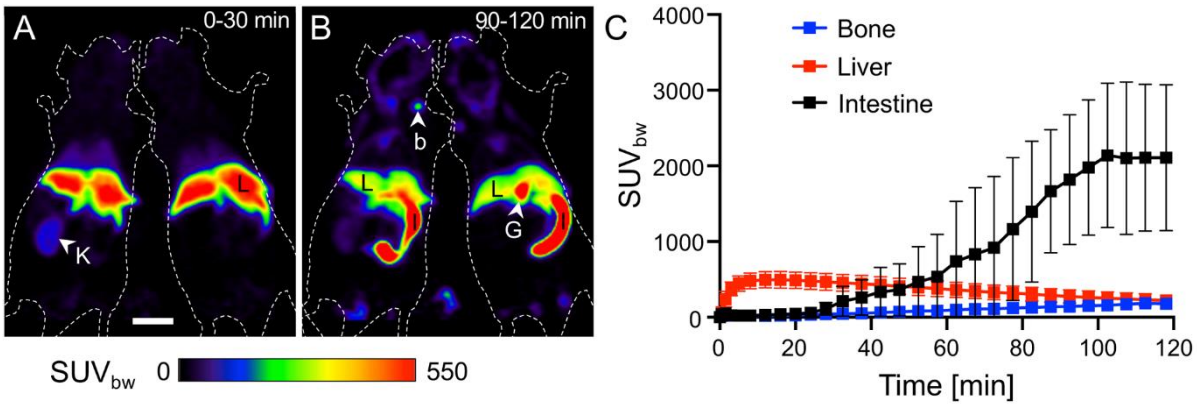

Figure 7. Evaluation of Boc-Tyr([^{18}F]SO_2F)-OMe ([^{18}F]**26**) in healthy mice (n=4) using µPET. Shown are summed images over 30 min of two individual mice in horizontal orientation. During the first 30 min (**A**), the tracer accumulated mainly in the liver, and was then released into the intestinal tract (**B**). Time-activity curves (**C**) demonstrated slow washout from the liver and high concentration in the intestine, reaching a plateau 100 min p.i. Abbreviations: b – bone (humeral head); G – gall bladder; I – intestine; K – kidney; L – liver. Scale bar: 1 cm.

Table 1. Biodistribution of Boc-Tyr([^{18}F]SO2F)-OMe ([^{18}F]**26**) from PET images in SUV_{bw} (mean±SD; n=4).

SUV_{bw}	30 min	60 min	90 min	120 min
brain	17.54 ± 4.96	7.71 ± 3.04	7.22 ± 2.86	7.64 ± 4.49
muscle (neck)	12.99 ± 3.43	12.66 ± 3.18	12.59 ± 2.97	11.69 ± 3.04
lung	57.56 ± 17.44	25.99 ± 9.18	21.69 ± 7.44	18.28 ± 6.57
heart	56.14 ± 14.62	33.56 ± 9.94	26.26 ± 8.32	21.35 ± 6.90
liver	474.27 ± 76.69	456.94 ± 82.15	354.75 ± 77.18	271.53 ± 66.96
gall bladder	361.58 ± 54.23	999.41 ± 503.25	1120.30 ± 528.42	1888.52 ± 1253.99

intestine	130.58 ± 129.31	775.42 ± 386.55	1673.83 ± 571.20	2042.63 ± 934.56
kidney	75.38 ± 28.51	49.22 ± 20.35	37.32 ± 17.05	28.70 ± 14.15
urinary bladder	12.19 ± 4.18	21.10 ± 8.48	25.65 ± 13.69	26.83 ± 14.24
bone (pelvis)	25.39 ± 5.65	60.50 ± 13.83	104.95 ± 27.44	155.34 ± 43.27

With an efficient procedure for SuFEx radiolabeling in hand, we next turned to the preparation of clinically relevant PET tracers. Radiolabeled amino acids can be used to visualize the upregulation of amino acid transporters and/or increased protein synthesis rates in peripheral and especially cerebral tumors [15,16]. For example, *O*-(2-[^{18}F]fluoroethyl)tyrosine ([^{18}F]FET) is widely used for the diagnosis of brain tumors [17]. Quite recently, we demonstrated how methylation of the carboxylic acid function can significantly increase the cerebral uptake of PET-tracers bearing an amino acid moiety [10]. With this in mind, we produced the methyl ester H-Tyr([^{18}F]SO_2F)-OMe ([^{18}F]**27**, prepared from 15 µg **27**) (**Fig. 6**) in the form of an injectable solution in an AY of 21% within 55 min and with excellent radiochemical purity. Similar to **1**, 1 µg of **27** (3.6 nmol) was sufficient to prepare the radiolabeled amino ester in good RCCs of 45±4% (**SI**, **Tab. S9**). The hydrolytic stability of [^{18}F]**27** in buffered media was evaluated in the pH range of 5.2–12 at ambient temperature (**SI**, **Fig. S39**). No defluorination of the tracer occurred at pH 8.9 or lower. At the same time, significant demethylation was observed at pH > 7. At pH 9.9, roughly half of the [^{18}F]**27** was hydrolyzed within 100 min and this was accompanied by mild defluorination (< 5% at the same time-point). At pH 12, the radiolabeled ester was completely hydrolyzed within 15 min, which was accompanied by a defluorination of approximately 37%. H-Tyr([^{18}F]SO_2F)-OMe was evaluated in rats bearing orthotopic U87 MG tumor xenografts (**Fig. 8**). These experiments demonstrated clear visualization of the tumors, with a signal-to noise ratio that amounted to 1.38±0.05 at 30–60 min p.i. Bone uptake during the 60 min measurement reached an SUV of 104±3.3, indicating defluorination on a level comparable to that of [^{18}F]FET. A more extensive preclinical evaluation of the novel tracer in comparison with [^{18}F]FET is ongoing and will be described in due course.

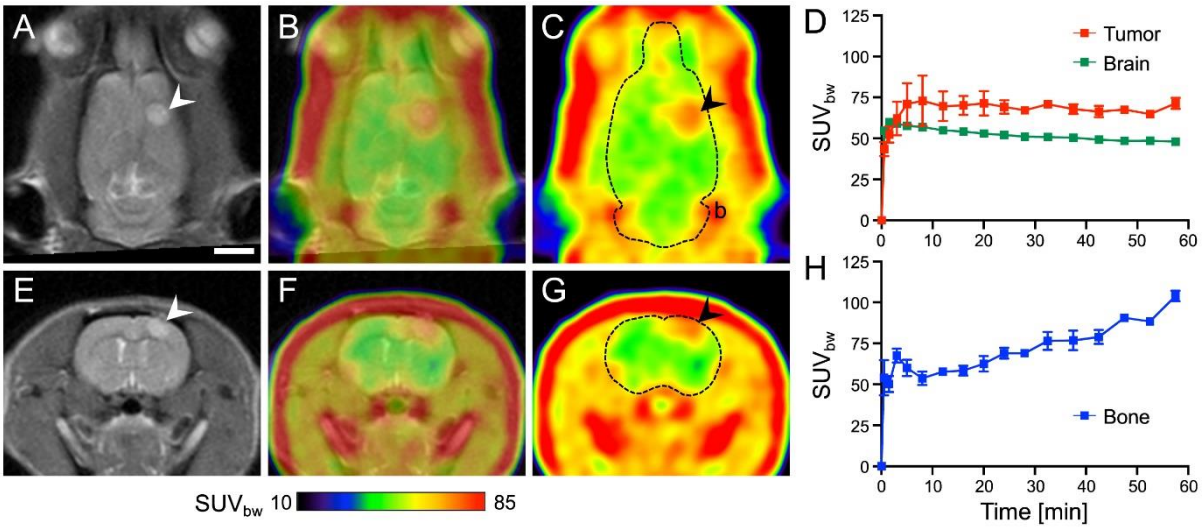

Figure 8. Visualization of U87 MG tumors in rats (n=2) by H-Tyr([^{18}F]SO_2F)-OMe-µPET. Shown are individual summed images (30–60 min p.i.) of one rat with corresponding MRI (T2) data in horizontal (**A**–**C**) and transverse (**E**–**G**) orientation. The tumor (arrowheads) was clearly visible against brain background. Time-activity curves (**D**+**H**) confirmed a stable tumor accumulation without any washout during the first 60 min p.i. Bone uptake increased steadily, but did not interfere with tumor detection. Abbreviations: b – bone (lambdoidal crest). Scale bar: 5 mm.

Fibroblast activation protein (FAP) is a membrane-bound serine protease that is overexpressed in the tumor microenvironment of >90% of all endothelial tumors but shows low expression in normal tissues [18,19]. As such, FAP undoubtedly represents one of the most promising targets for tumor imaging and, possibly, endoradiotherapy [20,21]. We therefore prepared **28**, an analog of UAMC1110, which is one of the most potent and selective FAP inhibitors [22]. **28** was then labeled using SuFEx radiofluorination in an AY of 47% within 40 min (**Fig. 6**). The molar activity amounted to 4.7 GBq/µmol (for 154 MBq tracer). [^{18}F]FS-UAMC1110 ([^{18}F]**28**) was subjected to a biological evaluation by µPET imaging in immunodeficient mice bearing subcutaneous fibrosarcoma tumors. Unexpectedly, hardly any radioactivity accumulation was observed in the tumors (maximum SUV_{bw} <30), neither in wildtype HT1080, nor in FAP-transfected HT1080-FAP tumors (**SI**, **Fig. S48**). Instead, the tracer accumulated strongly in the gall bladder (maximum SUV_{bw} 804±140, 90–120 min p.i.)(**SI**, **Tab. S11**). Furthermore, radioactivity uptake in bones (maximum SUV_{bw} 211±51, 90–120 min p.i.) demonstrated a higher defluorination rate of [^{18}F]**28**, which contains a [^{18}F]fluorosulfate group attached to an electron deficient 4-carboxamido substituted quinoline residue relative to the more electron rich aryl fluorosulfate-based tracers described above. This finding most likely indicates that highly electron deficient radiolabeled aryl fluorosulfates are not sufficiently stable for *in vivo* imaging applications.

DPA-714 is a selective agonist at the translocator protein 18 kDa (TSPO), a biomarker with relevance for different neurodegenerative and psychiatric diseases, stroke and brain tumors [23–25]. The corresponding radioligand [^{18}F]DPA-714 is widely used in preclinical and clinical TSPO PET studies. In the present work, [^{18}F]FS-DPA ([^{18}F]**29**, **Fig. 6**), a novel [^{18}F]DPA-714 analog that contains a radiolabeled fluorosulfate instead of the 2-[^{18}F]fluoroethoxy group, was prepared as an injectable solution in 42±3% AY within 25 min. Molar activity amounted to 3.5–7.9 GBq/µmol (128–317 MBq tracer). Visualization of neuroinflammation by [^{18}F]FS-DPA-PET was studied in a rat stroke model (**Fig. 9**). Ischemic stroke was induced by occlusion of the anterior cerebral artery (ACA) using stereotaxic injection of endothelin-1 [26]. ACA occlusion resulted in an ischemic lesion in the anterior cingulate cortex. 24 h after stroke induction, a T2-weighted MR image was acquired to visualize edema in the ACA territory, which should demarcate the area of subsequent neuroinflammation. At day 31 after stroke induction, the inflammatory processes were studied using [^{18}F]FS-DPA-PET images (0–120 min p.i.). As

illustrated in **Fig. 9**, the novel tracer reliably visualized neuroinflammation in the ACA territory. Maximum radioactivity uptake (SUV_{bw}) was 412±82 for [^{18}F]FS-DPA, 0–30 min p.i. After 2 h, SUV_{bw} still amounted to 260±53. The initial signal-to-noise ratio (SNR) of 3.1±0.5 at 0–30 min p.i. increased over time and amounted to 3.8±0.7 at 90–120 min p.i. [^{18}F]FS-DPA underwent fair defluorination with a cranial bone SUV_{bw} of 229±25 (90–120 min p.i.), which did not impede the image quality.

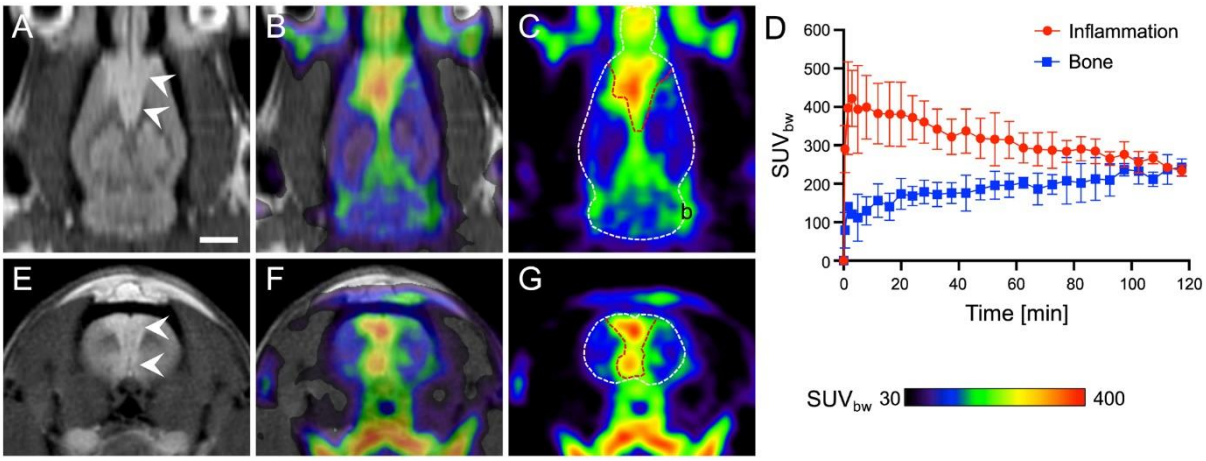

Figure 9. *In vivo* evaluation of [^{18}F]FS-DPA ([^{18}F]**29**) in a rat stroke model (n=3). Shown are individual summed images (30–60 min p.i.) of one rat with corresponding MRI (T2) data in horizontal (**A**–**C**) and transverse (**E**–**G**) orientation. MRI (T2) at 24 h post-stroke showed edema in the ACA territory (arrowheads in A+E). PET images (C+G) were taken 31 days after stroke, the region formerly affected by edema is indicated by a red outline. The time-activity curve (**D**) showed a slow washout of [^{18}F]FS-DPA from the inflammatory area, and a steadily increasing bone uptake.

3. Conclusion

We have established a robust protocol for the efficient preparation of radiolabeled aryl fluorosulfates via SuFEx ^{18}F/^{19}F isotopic exchange. Our optimized method overcomes problems associated with insufficient solubility of [^{18}F]KF/K_2CO_3/$K_{2.2.2}$ in the original procedure. In addition, the procedure circumvents time-consuming azeotropic drying steps and allows for the application of neutral salts instead of basic K_2CO_3. Our approach enables efficient radiolabeling using low nanomolar amounts of aryl fluorosulfates at micromolar concentrations. The versatility and scope of the radiofluorination method was demonstrated by the preparation of a series of 29 ^{18}F-labeled fluorosulfates, including analogs of complex compounds such as ezetimibe, α-tocopherol and etoposide, in fair to excellent yields. Preliminary evaluation demonstrated sufficient *in vivo* stability of radiolabeled electron rich or neutral aryl fluorosulfates. In contrast, electron deficient [^{18}F]FS-UAMC1110 suffered from a faster *in vivo* defluorination. Furthermore, [^{18}F]FS-DPA was identified as a promising imaging probe for visualization of TSPO under pathophysiological conditions. Taken together, the novel labeling protocol

demonstrated the enormous potential of SuFEx radiofluorination for accelerated development of novel PET tracers.

4. Experimental

4.1. General

Unless noted otherwise, all chemicals and solvents were purchased from VWR International (Radnor, PA, USA), Sigma-Aldrich (Steinheim, Germany), ChemPUR (Karlsruhe, Germany), ABCR GmbH (Karlsruhe, Germany) or Fluka AG (Buchs, Switzerland) and used without further purification. Fluorosulfonates **1**, **3**, **7**, **9**, **10**, **14**, **15** and **19–21** were acquired from Sigma-Aldrich (Steinheim, Germany). The purity of these compounds was checked by TLC and impure compounds were purified by column chromatography prior to use.

4.2. Nuclear magnetic resonance (NMR) spectroscopy

NMR-Spectra were measured at ambient temperature in deuterium oxide (D_2O), deuterochloroform ($CDCl_3$), deuteromethanol (CD_3OD), deuteroacetonitrile (CD_3CN), deuteroacetone [$(CD_3)_2CO$] or deuterodimethylsulfoxide [$(CD_3)_2SO$] as indicated using a Bruker Ascend™ 400 (^1H: 400 MHz; ^{13}C: 101 MHz; ^{19}F: 376 MHz). The measured chemical shifts are reported in δ [ppm] relative to residual peaks of non-deuterated solvents. The observed signal multiplicities are characterized as follows: s = singlet, s_b = broad singlet, d = doublet, t = triplet, m = multiplet and dd = doublet of doublet. Coupling constants *J* are reported in Hertz (Hz).

4.3. Mass spectrometry (MS)

Low resolution ESI mass spectra (LRMS-ESI) were measured with an MSQ PlusTM mass spectrometer (Thermo Electron Corporation, San Jose, USA). High resolution ESI mass spectra (HRMS-ESI) were measured with an LTQ XL™ Orbitrap™ (Thermo Fisher Scientific Inc., Bremen, Germany). High resolution EI mass spectra (HRMS-EI) were measured with an Exactive™ GC Orbitrap™ (Thermo Fisher Scientific Inc., Bremen, Germany).

4.4. Column chromatography

Manual column chromatography was performed with silica gel, 60 Å, 230–400 mesh particle size from Fluka AG (Buchs, Switzerland) or silica gel (w/Ca, 0.1%), 60 Å, 230–400 mesh particle size from Sigma-Aldrich GmbH (Steinheim, Germany). Automated column chromatography was either performed on a Grace Reverelis X1 (Columbia, Maryland, USA) or on a Büchi Pure C-815 Flash system, using Si60 FlashPure cartridges or Reveleris™ C_{18} reversed phase cartridges, respectively.

4.5. Thin layer chromatography (TLC)

TLC was performed using aluminum sheets coated with silica gel 0.25 mm SIL G/UV 254 (Merck KGaA, Darmstadt, Germany). Chromatograms were inspected under UV light (λ = 254 nm) and/or stained with phosphomolybdic acid (20% in EtOH).

4.6. High pressure liquid chromatography (HPLC)

HPLC analyses were carried out on a Dionex Ultimate® 3000 System with Ultimate® 3000 variable wavelength detector coupled in series with a Berthold LB500 NaI detector. Two Rheodyne 6 port injection valves equipped with equal sample loops were installed before and behind the chromatographic column. The UV and radioactivity detectors were connected in series, giving a time delay of 0.1–0.2 min between the corresponding responses, depending on the flow rate. Semi-preparative HPLC was performed on a dedicated semi-preparative system consisting of a Knauer K-100 pump, a Knauer K-2501 UV Detector, a Rheodyne 6 port injection valve equipped with a 2 mL injection loop and a custom-made Geiger counter. HPLC columns were purchased from Phenomenex (Aschaffenburg, Germany) and Merck KGaA (Darmstadt, Germany).

4.7. Determination of pH values

The pH values of aqueous solutions were measured with a 766 pH meter (Knick, Berlin, Germany) and an Inlab® Micro electrode (Mettler Toledo, Columbus, USA). The pH values of aqueous-organic mixtures were determined by spotting a small aliquot on pH 1–14 universal indicator paper (Merck KGaA, Darmstadt, Germany).

4.8. Chemistry

All reactions were carried out with magnetic stirring. Organic extracts were dried over anhydrous Na_2SO_4 or $MgSO_4$. Air or moisture sensitive reagents were handled under argon (>99.999%, Air Liquide GmbH). Solutions were concentrated under reduced pressure (1–900 mbar) at 40–50 °C using a rotary evaporator (Büchi Labortechnik, Essen, Germany). Solvent proportions are indicated in a volume/volume ratio.

3-Ethynylphenyl sulfurofluoridate (**2**) [5], 4-acetamidophenyl sulfurofluoridate (**5**), 2-*oxo*-*2H*-chromen-7-yl sulfurofluoridate (**11**) [27], 4-aminophenyl sulfurofluoridate (**16**) [27], 4-formyl-2-methoxyphenyl sulfurofluoridate (**18**) [27], *9H*-carbazol-2-yl sulfurofluoridate (**22**) [27], *N*,*N*-diethyl-2-{2-(4-hydroxyphenyl)-5,7-dimethylpyrazolo[1,5-a]pyrimidin-3-yl}-acetamide (*O*-desmethyl-DPA-713) (**S1**) [28] and (*S*)-1-(2-aminoacetyl)-4,4-difluoropyrrolidine-2-carbonitrile tosylate (**S2**) [22] were prepared according to the literature. 3-Methoxyphenyl sulfurofluoridate (**4**) [29], 3-formylphenyl

sulfurofluoridate (**6**) [30], 4-[(2-ethyl-1-benzofuran-3-yl)carbonyl]phenyl sulfurofluoridate (**8**), quinolin-8-yl sulfurofluoridate (**12**) [29], 3-*oxo*-3*H*-spiro[isobenzofuran-1,9'-xanthene]-3',6'-diyl bis(sulfurofluoridate) (**13**) [31], 2-amino-1,3-benzothiazol-5-yl sulfuro-fluoridate (**17**), 4-formyl-2-methoxyphenyl sulfurofluoridate (**18**) [32], ezetimibe (**23**), (±)-α-tocopherol (**24**) [32], and etoposide (**25**) derived sulfurofluoridates were prepared using AISF [27] according to **GP 1**.

4.8.1. Preparation of aryl sulfurofluoridates using AISF in CH_2Cl_2 – General Procedure 1 (**GP 1**)

DBU (164 µL, 0.167 g, 1.1 mmol, 2.2 eq) was added to a solution or suspension of the corresponding phenol (0.5 mmol, 1 eq.) in CH_2Cl_2 (4 mL). Thereafter, AISF (0.204 g, 0.65 mmol, 1.3 eq; in the case of etoposide derivative **25** 1.05 eq.) was added and the reaction mixture was stirred for 1–3 h. The reaction mixture was directly loaded onto the top of a column filled with dry silica and the desired aryl sulfurofluoridates were eluted with a suitable eluent. In the case of tocopherol derivative **24**, CH_2Cl_2 was removed under reduced pressure and the residue was taken up into hexane. Etoposide derivative **25** was not completely stable on silica. For the preparation of bis(sulfurofluoridate) **13**, 2.2 eq. AISF and 4.2 eq DBU were used.

4.8.2. Synthesis of 3-methoxyphenyl sulfurofluoridate (**4**) [29]

4 (0.19 g, 95%; colorless liquid) was prepared from 3-methoxyphenol according to **GP 1**. **Molecular formula and mass**: $C_7H_7FO_4S$ (206.187 g/mol). **^{1}H-NMR** [400 MHz, $CDCl_3$]: δ [ppm] = 7.37 (t, *J* = 8.3 Hz, 1H), 6.97 – 6.91 (m, 2H), 6.87 (td, *J* = 2.4, 0.8 Hz, 1H), 3.84 (s, 3H). **^{13}C-NMR** [101 MHz, $CDCl_3$]: δ [ppm] = 161.1, 150.9, 130.8, 114.6, 112.8, 107.1, 107.1, 55.9. **^{19}F-NMR** [376 MHz, $CDCl_3$]: δ [ppm] = 37.71 (s, 1F).

4.8.3. Synthesis of acetamidophenyl sulfurofluoridate (**5**)

Prepared as described for **26** below. Colorless solid. Yield: 92%. **Molecular formula and mass**: $C_8H_8FNO_4S$ (233.213 g/mol). **^{1}H-NMR** [400 MHz, $CDCl_3$]: δ [ppm] = 7.28–7.23 (d, *J* = 8.6 Hz, 2H), 7.44 (s_b, 1H, -NH), 7.29 (d, *J* = 8.7 Hz, 2H), 2.20 (s, 3H). **^{13}C-NMR** [101 MHz, $CDCl_3$]: δ [ppm] = 168.6, 145.9, 138.3, 121.7, 121.3, 24.7. **^{19}F-NMR** [376 MHz, $CDCl_3$]: δ [ppm] = 37.36 (s, 1F). **MS-ESI:** m/z $[M+H]^+$ calculated for $[C_8H_9FNO_4S]^+$ = 234.02, found 234.08.

4.8.4. Synthesis of 3-formylphenyl sulfurofluoridate (**6**) [30]

6 (58 mg, 23%; colorless liquid) was prepared from 3-hydroxybenzaldehyde according to **GP 1**. **Molecular formula and mass**: $C_7H_5FO_4S$ (204.171 g/mol). **^{1}H-NMR** [400 MHz, $CDCl_3$]: δ [ppm] = 10.05 (s, 1H), 7.95 (dt, *J* = 7.6, 1.2 Hz, 1H), 7.91 – 7.83 (m, 1H), 7.70 (t, *J* = 7.9 Hz, 1H), 7.62 (ddt, *J* = 8.2, 2.4, 0.9

Hz, 1H). **^{13}C-NMR** [101 MHz, $CDCl_3$]: δ [ppm] = 189.9, 150.6, 138.6, 131.5, 130.2, 126.8, 121.3. **^{19}F-NMR** [376 MHz, $CDCl_3$]: δ [ppm] = 38.48 (s, 1F).

4.8.5. Synthesis of 4-[(2-Ethyl-1-benzofuran-3-yl)carbonyl]phenyl sulfurofluoridate (**8**)

8 (0.17 g, 87%; colorless oil) was prepared from benzarone according to **GP 1**. **Molecular formula and mass**: $C_{17}H_{13}FO_5S$ (348.344 g/mol). **^{1}H-NMR** [400 MHz, $CDCl_3$]: δ [ppm] = 7.98 – 7.94 (m, 2H), 7.52 – 7.46 (m, 2H), 7.30 (dddd, *J* = 7.9, 5.6, 4.6, 1.4 Hz, 2H), 7.21 (ddd, *J* = 8.1, 7.1, 1.0 Hz, 1H), 2.94 (q, *J* = 7.5 Hz, 2H), 1.36 (t, *J* = 7.5 Hz, 3H). **^{13}C-NMR** [101 MHz, $CDCl_3$]: δ [ppm] = 189.9, 167.5, 153.8, 152.6, 139.7, 131.6, 126.5, 124.8, 124.0, 121.2, 121.2, 115.7, 111.4, 22.1, 12.4. **^{19}F-NMR** [376 MHz, $CDCl_3$]: δ [ppm] = 38.89 (s, 1F). **HRMS-ESI:** m/z $[M+H]^+$ calculated for $[C_{17}H_{14}FO_5S]^+$ = 349.05405, found: 349.05420.

4.8.6. Synthesis of quinolin-8-yl sulfurofluoridate (**12**) [29]

12 (0.12 g, 60%; colorless solid) was prepared from 8-hydroxyquinoline according to **GP 1**. **Molecular formula and mass**: $C_9H_6NFO_3S$ (227.209 g/mol). **^{1}H-NMR** [400 MHz, $CDCl_3$]: δ [ppm] = 9.07 (dd, *J* = 4.2, 1.6 Hz, 1H), 8.25 (dd, *J* = 8.4, 1.6 Hz, 1H), 7.90 (dd, *J* = 8.3, 1.2 Hz, 1H), 7.76 (dt, *J* = 7.7, 1.1 Hz, 1H), 7.63 – 7.57 (m, 1H), 7.55 (dd, *J* = 8.4, 4.2 Hz, 1H). **^{13}C-NMR** [101 MHz, $CDCl_3$]: δ [ppm] = 152.0, 146.0, 140.6, 136.1, 130.1, 128.8, 126.0, 122.9, 121.46. **^{19}F-NMR** [376 MHz, $CDCl_3$]: δ [ppm] = 40.66 (s, 1F). **MS-ESI:** m/z $[M+H]^+$ calculated for $[C_9H_7FNO_3S]^+$ = 228.01, found: 228.16.

4.8.7. Synthesis of 3-*oxo*-3*H*-spiro[isobenzofuran-1,9'-xanthene]-3',6'-diyl bis(sulfurofluoridate) (**13**) [31]

13 (84 mg, 42%; colorless solid) was prepared from fluorescein according to **GP 1**. **Molecular formula and mass**: $C_{20}H_{10}F_2O_9S_2$ (496.408 g/mol). **^{1}H-NMR** [400 MHz, $CDCl_3$]: δ [ppm] = 8.11 – 8.05 (m, 1H), 7.72 (dqd, *J* = 14.6, 7.4, 1.2 Hz, 2H), 7.37 (d, *J* = 2.4 Hz, 2H), 7.21 – 7.15 (m, 1H), 7.11 (ddd, *J* = 8.8, 2.5, 0.6 Hz, 2H), 7.00 (d, *J* = 8.8 Hz, 2H). **^{13}C-NMR** [101 MHz, $CDCl_3$]: δ [ppm] = 168.6, 152.3, 151.5, 150.7, 136.0, 130.9, 130.3, 125.9, 125.7, 123.9, 119.8, 117.4, 110.5, 80.1. **^{19}F-NMR** [376 MHz, $CDCl_3$]: δ [ppm] = 38.80 (s, 2F). **MS-ESI:** m/z $[M+H]^+$ calculated for $[C_{20}H_{11}F_2O_9S_2]^+$ = 496.98, found: 497.04.

4.8.8. Synthesis of 2-amino-1,3-benzothiazol-5-yl sulfurofluoridate (**17**)

17 (48 mg, 29%; colorless solid) was prepared from 2-amino-5-hydroxy-1,3-benzothiazole according to **GP 1**. **Molecular formula and mass**: $C_7H_5FN_2O_3S_2$ (248.246 g/mol). **^{1}H-NMR** [400 MHz, $(CD_3)_2CO$]: δ [ppm] = 7.89 (d, *J* = 2.0 Hz, 1H), 7.50 (d, *J* = 8.8 Hz, 1H), 7.38 (ddd, *J* = 8.8, 2.6, 1.0 Hz, 1H), 7.13 (s_b, 2H). **^{13}C-NMR** [101 MHz, $(CD_3)_2CO$]: δ [ppm] = 169.3, 154.2, 145.2, 133.8, 119.8, 119.4, 114.8. **^{19}F-**

NMR [376 MHz, $(CD_3)_2CO$]: δ [ppm] = 35.43 (s, 1F). **HRMS-ESI:** m/z $[M+H]^+$ calculated for $[C_7H_6FN_2O_3S_2]^+$ = 248.97984, found: 248.98000.

4.8.9. Synthesis of 4-formyl-2-methoxyphenyl sulfurofluoridate (**18**) [32]

18 (0.11 g, 71%; colorless solid) was prepared from vanillin according to **GP 1**. **Molecular formula and mass**: $C_8H_7FO_5S$ (234.197 g/mol). **^{1}H-NMR** [400 MHz, $CDCl_3$]: δ [ppm] = 10.00 (s, 1H), 7.59 (d, *J* = 1.3 Hz, 1H), 7.55 – 7.49 (m, 2H), 4.01 (s, 3H). **^{13}C-NMR** [101 MHz, $CDCl_3$]: δ [ppm] = 190.5, 152.2, 142.9, 137.2, 124.1, 123.3, 112.2, 56.7. **^{19}F-NMR** [376 MHz, $CDCl_3$]: δ [ppm] = 41.02 (s, 1F).

4.8.10. Synthesis of ezetimibe-derived sulfurofluoridate (**23**)

23 (0.16 g, 67%; colorless solid) was prepared from ezetimibe according to **GP 1**. **Molecular formula and mass**: $C_{24}H_{20}F_3NO_5S$ (491.481 g/mol). **^{1}H-NMR** [400 MHz, $CDCl_3$]: δ [ppm] = 7.46 – 7.41 (m, 2H), 7.36 (d, *J* = 8.5 Hz, 2H), 7.32 – 7.26 (m, 2H), 7.23 – 7.17 (m, 2H), 7.06 – 6.99 (m, 2H), 6.99 – 6.92 (m, 2H), 4.72 (t, *J* = 6.1 Hz, 1H), 4.68 (d, *J* = 2.3 Hz, 1H), 3.07 (td, *J* = 7.6, 2.3 Hz, 1H), 2.27 (s, *J* = 10.7 Hz, 1H), 2.11 – 1.84 (m, 4H). **^{13}C-NMR** [101 MHz, $CDCl_3$]: δ [ppm] = 167.0, 162.4 (d, *J* = 245.9 Hz), 159.3 (d, *J* = 244.2 Hz), 149.9, 140.0 (d, *J* = 3.0 Hz), 138.7, 133.6 (d, *J* = 2.7 Hz), 128.0, 127.5 (d, *J* = 8.0 Hz), 122.1, 118.4 (d, *J* = 7.9 Hz), 116.2 (d, *J* = 22.7 Hz), 115.6 (d, *J* = 21.2 Hz), 73.3, 60.8, 60.5, 36.7, 25.2. **^{19}F-NMR** [376 MHz, $CDCl_3$]: δ [ppm] = 38.03 (s, 1F), -114.63 (s, 1F), -117.30 (s, 1F). **HRMS-ESI:** m/z $[M+Na]^+$ calculated for $[C_{24}H_{20}F_3NO_5SNa]^+$ = 514.09065, found: 514.09065.

4.8.11. Synthesis of (±)-α-tocopherol-derived sulfurofluoridate (**24**) [32]

24 (0.25 g, 84%; colorless oil) was prepared from (±)-α-tocopherol according to **GP 1**. **Molecular formula and mass**: $C_{29}H_{49}FO_4S$ (512.765 g/mol). **^{1}H-NMR** [400 MHz, $CDCl_3$]: δ [ppm] = 2.60 (t, *J* = 6.8 Hz, 2H), 2.24 (s, 3H), 2.20 (s, 3H), 2.11 (s, 3H) , 1.90 – 1.72 (m, 2H), 1.63 – 1.02 (m, 25H), 0.90 – 0.82 (m, 12H). **^{13}C-NMR** [101 MHz, $CDCl_3$]: δ [ppm] = 151.2, 142.0, 127.7, 126.2, 124.5, 118.6, 75.9, 40.1, 40.1, 39.5, 37.7, 37.6, 37.6, 37.5, 37.5, 37.4, 33.0, 32.9, 32.8, 32.8, 31.0, 30.9, 28.1, 25.0, 25.0, 24.6, 24.0, 22.9, 22.8, 21.1, 20.8, 19.9, 19.8, 19.8, 19.8, 19.8, 13.7, 13.7, 12.9, 12.8, 12.1. **^{19}F-NMR** [376 MHz, $CDCl_3$]: δ [ppm] = 41.36 (s, 1F).

4.8.12. Synthesis of etoposide-derived sulfurofluoridate (**25**)

25 (25 mg, 17%; colorless foam) was prepared from etoposide according to **GP 1**. **Molecular formula and mass**: $C_{29}H_{31}FO_{15}S$ (670.610 g/mol). **^{1}H-NMR** [400 MHz, CD_3CN]: δ [ppm] = 7.07 (s, 1H), 6.66 (s, 2H), 6.41 (s, 1H), 5.95 (s, 2H), 4.78 (d, *J* = 4.5 Hz, 1H), 4.71 (q, *J* = 5.0 Hz, 1H), 4.41 (d, *J* = 5.5 Hz, 1H), 4.39 – 4.31 (m, 2H), 4.24 (d, *J* = 7.8 Hz, 1H), 4.09 – 4.03 (m, 1H), 3.85 (s, 6H), 3.56 – 3.47 (m, 3H), 3.42 (d, *J* = 4.2 Hz, 1H), 3.38 (dd, *J* = 8.6, 4.2 Hz, 1H), 3.24 – 3.14 (m, 4H), 1.26 (d, *J* = 5.0 Hz, 3H). **^{13}C-NMR**

[101 MHz, CD_3CN]: δ [ppm] = 179.8, 153.3, 148.9, 147.5, 145.4, 133.0, 130.0, 109.8, 109.0, 106.8, 102.6, 102.0, 100.1, 81.0, 76.1, 75.5, 74.2, 69.4, 68.7, 67.1, 57.4, 45.9, 44.0, 40.0, 20.7. **^{19}F-NMR** [376 MHz, CD_3CN]: δ [ppm] = 42.43 (s, 1F). **HRMS-ESI:** m/z $[M+H]^+$ calculated for $[C_{29}H_{31}FO_{15}SNa]^+$ = 693.12599, found: 693.12579.

4.8.13. Synthesis of methyl (*S*)-2-[(*tert*-butoxycarbonyl)amino]-3-{4-[(fluorosulfonyl)oxy]phenyl}propanoate (Boc-Tyr(FS)-OMe, **26**)

1,8-Diazabicyclo[5.4.0]undec-7-en (0.891 mL, 0.907 g, 5.96 mmol) was added to a solution of Boc-Tyr-OMe (0.8 g, 2.71 mmol) and [4-(acetylamino)phenyl]imidodisulfuryl difluoride (AISF) [27] (1.022 g, 3.25 mmol) in THF (12.5 mL) and the reaction mixture was vigorously stirred for 10 min. The resulting heterogeneous mixture was taken up in 100 mL Et_2O/H_2O (1:1), the organic layer was separated and successively washed with 1 M $NaHSO_4$ (3×20 mL), H_2O (2×20 mL), 5% $NaHCO_3$ (3×20 mL) and brine (2×20 mL). That followed, the organic layer was concentrated under reduced pressure, the residue was taken up in EtOAc/hexane (1:2.5) and filtered through a pad of silica (10 g). The resulting solution was concentrated under reduced pressure and the residue was recrystallized from pentane (–25 °C) to afford the title compound (0.92 g, 90%) as a colorless solid. **Molecular formula and mass**: $C_{15}H_{20}FNO_7S$ (377.383 g/mol). **^{1}H-NMR** [400 MHz, $CDCl_3$]: δ [ppm] = 7.28–7.23 (m, 4H), 5.04–4.79 (m, 1 H, -NH), 4.63–4.41 (m, 1H), 3.72 (s, 3H), 3.18 (dd, *J* = 13.9, 5.6 Hz, 1H), 3.04 (d, *J* = 13.8, 6.5 Hz, 1H), 1.40 (s, 9H). **^{13}C-NMR** [101 MHz, $CDCl_3$]: δ [ppm] = 172.0, 155.1, 149.2, 137.4, 131.4, 121.0, 80.4, 54.3, 52.6, 38.0, 28.4. **^{19}F-NMR** [376 MHz, $CDCl_3$]: δ [ppm] = 37.48 (s, 1F). **MS-ESI:** m/z $[M-Boc+H]^+$ calculated for $[C_{10}H_{14}FNO_5S]^+$ = 278.05, found: 278.10. ***R*$_f$ value**: R_f = 0.36 (EtOAc/hexane = 1:2.5).

4.8.14. Synthesis of methyl (*S*)-2-amino-3-{4-[(fluorosulfonyl)oxy]phenyl}propanoate hydrochloride (H-Tyr(FS)-OMe·HCl, **27**·HCl)

MeOH (20 µL, 16 mg, 0.50 mmol, 5.0 eq.) was slowly added to an ice-cold solution of AcCl (35 µL, 38 mg, 0.48 mmol, 4.8 eq.) in EtOAc (1 mL) and the mixture was stirred for 5 min. **26** (38 mg, 100 µmol, 1.0 eq.) was then added, the cooling bath was removed and the reaction mixture was stirred for 30 min. After completion of the reaction, the mixture was concentrated under reduced pressure to afford the title compound as a colorless solid (96% yield, 30 mg, 96 µmol). **Molecular formula and mass**: $C_{10}H_{13}ClFNO_5S$ (313.724, free base: 277.266 g/mol). **^{1}H-NMR** [400 MHz, D_2O]: *δ* [ppm] = 7.55–7.46 (m, 4H), 4.48 (dd, *J* = 7.4, 6.2 Hz, 1H), 3.85 (s, $-NH_3^+$ and HOD, 4H), 3.42 (dd, *J* = 14.6, 6.2 Hz, 1H), 3.33 (dd, *J* = 14.6, 7.5 Hz, 1H). **^{13}C-NMR** [101 MHz, D_2O]: *δ* [ppm] = 169.9, 149.5, 135.1, 131.6, 121.6, 53.8, 53.6, 35.0. **^{19}F-NMR** [376 MHz, D_2O]: *δ* [ppm] = 37.53 (s, 1F). **HRMS-ESI:** m/z $[M+H]^+$ calculated for $[C_{10}H_{13}FNO_5S]^+$ = 278.04930, found: 278.04936, m/z $[M+Na]^+$ calculated for $[C_{10}H_{12}FNO_5SNa]^+$ = 300.03124, found 300.03135.

4.8.15. Synthesis of (*S*)-4-{[2-(2-Cyano-4,4-difluoropyrrolidin-1-yl)-2-oxoethyl]carbamoyl}quinolin-6-yl sulfurofluoridate (**28**)

a) Methyl 6-iodoquinoline-4-carboxylate (**S3**)

Sodium pyruvate (2.42 g, 22.0 mmol, 1.2 eq.) was added to a solution of 5-iodoisatine (5.00 g, 18.3 mmol) in 20% aqueous NaOH (36 mL, 12 eq.) and the reaction mixture was stirred under reflux until gas evolution had ceased (4 h). The reaction mixture was vigorously stirred and diluted with water (25 mL), cooled with a water-ice bath and neutralized with 12 M HCl (about 20.5 mL) to pH=2. The resulting suspension was stirred for 1 h, after which the precipitate was collected by filtration, rinsed with water (2×20 mL), MeOH (15 mL) and Et_2O (150 mL), and dried under reduced pressure to afford 4.70 g (75%) of crude 6-iodo-quinoline-2-4-dicarboxylic acid, which was used for the subsequent decarboxylation step without further purification. The crude diacid (4.70 g, 13.7 mmol) was placed in a 250 mL 3-neck round bottom flask equipped with a stirring bar, a gas inlet, and a distilling bridge connected to a Schlenk flask that was chilled with crushed ice. Nitromethane (90 mL) was added with stirring and the reaction mixture was brought to vigorous boiling until 7–10 mL of the nitromethane had been distilled off at ambient pressure. The reaction mixture was allowed to cool down in a gentle stream of argon, the bridge was replaced by a reflux condenser, and the mixture was heated under reflux for another 20 min. Thereafter, it was cooled down to ambient temperature, diluted with CH_2Cl_2 (50 mL) and stirred for 1 h. The resulting precipitate was collected by filtration, washed with CH_2Cl_2 (3×15 mL), and dried under reduced pressure to give 3.82 g (94%) of crude 6-iodo-quinoline-4-dicarboxylic acid as an off-white solid. The product could be purified by sublimation, which furnished a colorless solid but was associated with significant losses, so that the subsequent esterification step was typically performed without prior purification. **Molecular formula and mass**: $C_{10}H_6INO_2$ (299.067 g/mol). **^{1}H-NMR** [400 MHz, $(CD_3)_2SO$]: δ [ppm] = 13.97 (s, 1H), 9.18 (d, *J* = 1.3 Hz, 1H), 9.05 (d, *J* = 4.3 Hz, 1H), 8.08 (dd, *J* = 8.8, 1.6 Hz, 1H), 7.97 (d, *J* = 4.3 Hz, 1H), 7.87 (d, *J* = 8.8 Hz, 1H). **^{13}C-NMR** [101 MHz, $(CD_3)_2SO$]: δ [ppm] = 167.0, 151.1, 147.3, 138.1, 134.2, 134.1, 131.5, 126.1, 123.04, 95.3, 39.5. **MS-ESI:** m/z $[M+H]^+$ calculated for $[C_{10}H_7INO_2]^+$ = 299.95, found 300.02, m/z $[M-H]^-$ calculated for $[C_{10}H_5INO_2]^-$ = 297.94, found: 297.99.

Oxalyl chloride (5.00 mL, 3.38 g, 26.6 mmol, 1.8 eq.) was added to an ice-cold suspension of the crude 6-iodo-quinoline-4-dicarboxylic acid (4.50 g, 15.0 mmol, 1.0 eq.) in CH_2Cl_2 (10 mL). The cooling bath was removed and the reaction mixture was stirred for 3 h. Thereafter, $C_2H_4Cl_2$ (20 mL) was added and the mixture was gradually heated to 65 °C over 2 h. The reaction mixture was allowed to cool to ambient temperature and stirred for 16 h, after which it was cooled in a water-ice bath and MeOH (3.0 mL, 2.4 g, 74 mmol, 2.8 eq.) followed by Et_3N (7.0 mL, 5.1 g, 50 mmol, 1.9 eq.) were added. The cooling bath was removed, the reaction mixture was stirred for 2 h and then concentrated under

reduced pressure. The residue was dissolved in hot EtOAc and the resulting solution filtered through Celite™. The filter cake was rinsed with fresh EtOAc and the combined filtrates were washed with 1 M citric acid, H_2O, 10% $NaHCO_3$, and brine. After drying of the organic phase and removal of EtOAc under reduced pressure, the residue was recrystallized from MeCN to afford **S3** (72%, 3.36 g, 10.7 mmol) as a colorless solid. **Molecular formula and mass**: $C_{11}H_8INO_2$ (313.094 g/mol). **^{1}H-NMR** [400 MHz, $CDCl_3$]: δ [ppm] = 9.24 (d, J = 1.9 Hz, 1H), 9.02 (d, J = 4.4 Hz, 1H), 8.02 (dd, J = 8.9, 1.9 Hz, 1H), 7.92 (d, J = 4.4 Hz, 1H), 7.88 (d, J = 8.9 Hz, 1H), 4.05 (s, 3H). **^{13}C-NMR** [101 MHz, $CDCl_3$]: δ [ppm] = 166.2, 150.4, 148.2, 138.9, 134.8, 133.6, 131.6, 126.7, 123.0, 92.5, 53.1. **MS-ESI:** m/z $[M+H]^+$ calculated for $[C_{11}H_9INO_2]^+$ = 313.97, found 314.02. **DIP-HRMS-EI** (70 eV, 50 °C): m/z $[M]^{\cdot+}$ calculated for $[C_{10}H_6INO_2]^{\cdot+}$ = 312.95942, found: 312.95898.

b) 6-(4,4,5,5-Tetramethyl-1,3,2-dioxaborolan-2-yl)quinoline-4-carboxylic acid methyl ester (**S4**)

Anhydrous potassium acetate (1.47 g, 15.0 mmol, 3.0 eq.) was added to a solution of 6-iodoquinoline-4-carboxylic acid methyl ester (**S3**) (1.57 g, 5.01 mmol), $Pd(dppf)Cl_2$ (0.15 mmol, 92 mg, 2.5 mol%), and bis(pinacolato)diboron (1.40 g, 5.50 mmol, 1.1 eq.) in anhydrous DMF (25 mL) and the resulting suspension was vigorously stirred under argon at 70 °C for 12 h. The reaction mixture was cooled to ambient temperature, diluted with Et_2O (100 mL) and filtered through a 2-cm plug of Celite™. The filter cake was rinsed with Et_2O (2 × 50 mL) and the combined filtrates were concentrated under reduced pressure at T_{bath} <45 °C until most of the DMF had distilled off (condensation of DMF ceased when the internal pressure reached 6–8 mbar) to afford the crude product as a dark-brown solid. Subsequent fractional distillation in a Kugelrohr apparatus at 80–150 °C/0.1–1 mbar gave the following fractions: 1) b.p. 80–100 °C/1 mbar: 0.49 g of a colorless crystalline material [predominantly $(Bpin)_2$ + **S4** <2% + **S3** <12%] which was discarded, and 2) b.p. 110–150 °C/0.1–1 mbar: 1.20 g of the title compound (77% yield) as a pale-yellow thick oil, which gradually solidified at ambient temperature. As its NMR-spectrum confirmed sufficient purity, the product was directly used without further purification. **Molecular formula and mass**: $C_{17}H_{20}BNO_4$ (313.160 g/mol). **^{1}H-NMR** [400 MHz, $CDCl_3$]: δ [ppm] = 9.17 (s, 1H), 9.04 (d, J = 4.4 Hz, 1H), 8.16–8.11 (m, 2H), 7.86 (d, J = 4.4 Hz, 1 H), 4.06 (s, 3 H), 1.39 (s, 12 H). **^{13}C-NMR** [101 MHz, $CDCl_3$]: δ [ppm] = 166.7, 150.8, 150.5, 135.8, 134.7, 133.5, 129.1, 124.5, 122.1, 84.4, 52.9, 25.1, missing: $C_{arom.}$–Bpin. **MS-ESI:** m/z $[M+H]^+$ calculated for $[C_{17}H_{21}BNO_4]^+$ = 314.16, found 314.24. **DIP-HRMS-EI** (70 eV, 50–115 °C): m/z $[M]^{\cdot+}$ calculated for $[C_{17}H_{20}BNO_4]^{\cdot+}$ = 313.14799, found: 313.14766.

c) 6-(4,4,5,5-Tetramethyl-[1,3,2]dioxaborolan-2-yl)-quinoline-4-carboxylic acid (**S5**)

A solution of **S4** (361 mg, 1.15 mmol) and anhydrous TMSOK (325 mg, 2.54 mmol, 2.2 eq.) in anhydrous THF (5 mL) was stirred for 4 h, after which all volatiles were removed under reduced pressure

to afford a free-flowing pale-creamy powder. Following addition of 2,3,5,6-tetrafluorophenol (TFP-OH) (0.422 g, 2.54 mmol, 2.2 eq.) and anhydrous THF (5 mL), the reaction mixture was stirred for 1 h and concentrated under reduced pressure. After a subsequent drying step at 25 °C/0.01 mbar for 1 h, the residue was dissolved in anhydrous Et_2O (10 mL) and stirred until precipitation of the product from the reaction mixture was complete. The colorless precipitate was collected by filtration, washed with Et_2O (2×10 mL) and dried under reduced pressure to afford the title compound as a colorless free-flowing powder (308 mg, 79% yield). **Molecular formula and mass**: $C_{16}H_{18}BNO_4$ (299.133 g/mol). **^{1}H-NMR** [400 MHz, $(CD_3)_2CO$]: δ [ppm] = 8.93 (dd, J = 1.4, 0.8 Hz, 1H), 8.77 (d, J = 4.3 Hz, 1H), 7.88 (dd, J = 8.4, 0.8 Hz, 1H), 7.83 (dd, J = 8.4, 1.4 Hz, 1H), 7.33 (d, J = 4.3 Hz, 1H), 1.34 (s, 12H). **^{13}C-NMR** [101 MHz, $(CD_3)_2CO$]: δ [ppm] = 172.6, 152.2, 151.2, 148.3, 137.2, 133.6, 129.2, 126.3, 121.4, 84.7, 25.2, missing: $C_{arom.}$–Bpin. **HRMS-ESI:** m/z $[M+H]^+$ calculated for $[C_{16}H_{19}BNO_4]^+$ = 300.14017, found 300.14042, $[C_{16}H_{18}BNO_4Na]^+$ = 322.12211, found: 322.1221.

d) 6-(4,4,5,5-Tetramethyl-[1,3,2]dioxaborolan-2-yl)-quinoline-4-carboxylic acid 2,3,5,6-tetrafluorophenyl ester (**S6**)

A solution of **S5** (287 mg, 0.960 mmol), EDC (202 mg, 1.05 mmol, 1.1 eq.) and TFP-OH (310 mg, 1.87 mmol, 2.0 eq.) in anhydrous CH_2Cl_2 (10 mL) was stirred for 16 h. After concentration under reduced pressure and trituration of the residue with a mixture of EtOAc (30 mL) and H_2O (20 mL), the aqueous phase was extracted with EtOAc (2×20 mL), and the extract was washed with H_2O (2×10 mL) and brine (30 mL). The organic phase was then dried and volatiles were removed under reduced pressure to afford the crude active ester **S6** (404 mg, corresponding to 312 mg of the pure compound, as estimated from its ^{1}H-spectrum that showed TFP-OH as the only visible impurity), which was used for the next step without further purification (^{1}H-NMR-spectra of the crude product showed no impurities other than TFP-OH (approx. 0.8 eq.), which does not interfere with the following step and is completely removed during lyophilic drying of the final product **S7**). **Molecular formula and mass**: $C_{22}H_{18}BF_4NO_4$ (447.193 g/mol). **^{1}H-NMR** [400 MHz, $CDCl_3$]: δ [ppm] = 9.29 (m, 1H), 9.16 (d, J = 4.5 Hz, 1H), 8.29–8.17 (m, 3H), 7.12 (s, 1H, 4'-H of TFP-ester), 6.61 (s, 1H, 4'-H of free TFP-OH), 1.38 (s, 12H).

e) 6-(1,1-Dihydroxyboryl)-quinoline-4-carboxylic acid [2-(2-cyano-4,4-difluoro-pyrrolidin-1-yl)-2-oxoethyl]-amide (**S7**)

Anhydrous Et_3N (310 µL, 225 mg, 2.22 mmol, 3.2 eq.) was added dropwise and with stirring to an ice-cold solution of crude **S6** (404 mg crude, 312 mg, 0.70 µmol) and (*S*)-1-(2-amino-acetyl)-4,4-difluoro-pyrrolidine-2-carbonitrile tosylate (**S2**) (290 mg, 0.80 mmol, 1.1 eq.) in anhydrous CH_2Cl_2 (3.5 mL). When the addition was complete, the cooling bath was removed and the reaction mixture was stirred for another 16 h. After subsequent concentration of the mixture under reduced pressure, the

residue was triturated with EtOAc (15 mL) and a mixture of H_2O (8 mL), brine (0.5 mL) and 1 N HCl (1.5 mL). The aqueous fraction was extracted with EtOAc (3×10 mL) and the combined extracts were washed with H_2O (3×10 mL) and brine (15 mL). The residue obtained after drying of the organic fraction and removal of volatiles under reduced pressure was dissolved in CH_2Cl_2 and concentrated under reduced pressure to afford, after an additional drying step in high vacuum, an off-white foam which contained 6-(4,4,5,5-tetramethyl-[1,3,2]dioxaborolan-2-yl)-quinoline-4-carboxylic acid (*S*)-[2-(2-cyano-4,4-difluoro-pyrrolidin-1-yl)-2-oxo-ethyl]-amide **S6** and PFP-OH (487 mg of 1:1.9 mixture of **S6** and TFP-OH according to ^{1}H-NMR and ^{19}F-NMR-spectra, which corresponds to approximately 285 mg of the pure intermediate **S6**). Since the pinacol boronic ester readily undergoes decomposition during purification by normal or reverse-phase chromatography, it was converted into the corresponding boronic acid as follows. The crude pinacol boronic ester was dissolved in hot 40% MeOH (100 mL) and the resulting solution was completely evaporated under reduced pressure (T_{bath} 40-45 °C; three times). Thereafter, the residue was dissolved in hot MeOH (10 mL), the resulting solution was heated to reflux, and H_2O (approx. 120 mL) was added with stirring until a slight turbidity could be observed. After 30 min, heating was stopped, activated charcoal (210 mg) was added, and the mixture was allowed to return to ambient temperature. The solution was then filtered through a thin plug of Celite™, the filter cake was washed with 10% MeOH (2×10 mL), and the combined filtrates were concentrated under reduced pressure to a volume of approximately 50 mL. The resulting solution was frozen by occasional swirling in a liquid nitrogen bath and lyophilized ($T_{cond.}$ -90 °C, P = 0.2 mbar, 24 h) to afford, after an additional drying step in a vacuum-desiccator over Sicapent™ at 20 °C/0.01 mbar overnight, 203 mg (75%) of >92% pure (as estimated from its ^{1}H-NMR-spectrum) product **S7** as a colorless free-flowing powder. **Molecular formula and mass**: $C_{17}H_{15}BF_2N_4O_4$ (388.138 g/mol). **^{1}H-NMR** [400 MHz, $(CD_3)_2SO$]: δ [ppm] = 8.94 (d, *J* = 3.6 Hz, 1H), 8.70 (s, 1H), 8.07 (dd, *J* = 18.6, 7.3 Hz, 2H), 7.67 (d, *J* = 4.4 Hz, 1H), 5.54 (d, *J* = 9.1 Hz, 0.13 H, min.) and 5.17 (dd, *J* = 9.3, 2.8 Hz, 0.91 H, maj.), 4.44 – 4.10 (m, 4H), 3.03 – 2.76 (m, 2H). **^{13}C-NMR** [101 MHz, $(CD_3)_2SO$]: δ [ppm] = 170.4, 169.5, 151.4, 144.2, 136.0, 128.3, 127.6 (dd, *J* = 251, 247 Hz), 120.3, 118.1, 53.0 (t, *J* = 33 Hz), 45.8 (d, *J* = 6 Hz), 42.9, 38.2 (t, *J* = 25 Hz). **^{19}F-NMR** [376 MHz, $(CD_3)_2SO$]: δ [ppm] = -96.63 – -98.55 (m, 1 F), -105.19 – -108.38 (m, 1 F). **HRMS-ESI:** m/z $[M+H]^+$ calculated for $[C_{17}H_{16}BF_2N_4O_4]^+$ = 389.12272, found: 389.12203. ***R*$_f$ value**: R_f = 0.11 (EtOAc).

f) (*S*)-*N*-[2-(2-Cyano-4,4-difluoropyrrolidin-1-yl)-2-oxoethyl]-6-hydroxyquinoline-4-carboxamide (**S8**)

m-CPBA (30 mg, max. 77% purity, approx. 130 µmol, 1.3 eq.) was added to an ice-cold solution of **S7** (39 mg, 100 µmol, 1.0 eq.) in EtOH/H_2O (2:1; 1.5 mL), the cooling bath was removed and the reaction mixture was stirred for 6 h and stored at 4 °C overnight. On the next day, the reaction mixture was

diluted with H_2O (4 mL) and extracted with EtOAc (5×10 mL). The combined organic phases were dried and concentrated under reduced pressure to afford the crude product **S8** (44 mg). Half of the crude product (22 mg) was directly used for the synthesis of **28**, while the rest was purified by column chromatography (EtOAc) to afford analytically pure **S8** (13 mg, 36 µmol, 36%) as a colorless solid. **Molecular formula and mass**: $C_{17}H_{14}F_2N_4O_3$ (360.1034 g/mol). **^{1}H-NMR** [400 MHz, CD_3CN/CD_3OD]: δ [ppm] = 8.72 (d, *J* = 4.4 Hz, 1 H), 7.98 (d, *J* = 9.1 Hz, 1 H), 7.62 (d, *J* = 2.7 Hz, 1 H), 7.54 (d, *J* = 4.4 Hz, 1 H), 7.41 (dd, *J* = 9.1, 2.7 Hz, 1 H), 5.40–5.11 (m, 1 H), 4.54–4.08 (m, 4 H), 2.98–2.77 (m, 2 H). **^{13}C-NMR** [101 MHz, CD_3CN/CD_3OD]: δ [ppm] = 170.1, 169.5, 157.8, 147.6, 144.6, 141.6, 131.3, 127.6 (dd, *J* = -250.8, -246.6 Hz), 127.3, 123.8, 120.5, 118.2, 107.4, 52.9 (m), 45.7 (d, *J* = 6.0 Hz), 42.8, 38.0 (t, *J* = 32.2 Hz), 25.2. **^{19}F-NMR** [376 MHz, CD_3CN/CD_3OD]: δ [ppm] = -94.81 – -96.77 (m, 1 F), -103.83 – -106.83 (m, 1F). **MS-ESI:** m/z $[M+H]^+$ calculated for $[C_{17}H_{15}F_2N_4O_3]^+$ = 361.11, found: 361.12. **DIP-HRMS-EI** (70 eV, 50 –260 °C): m/z $[M]^{\cdot+}$ calculated for $[C_{17}H_{14}F_2N_4O_3]^{\cdot+}$ = 360.10285, found: 360.10252. ***R*$_f$ value**: R_f = 0.15 (EtOAc).

g) (*S*)-4-{[2-(2-Cyano-4,4-difluoropyrrolidin-1-yl)-2-oxoethyl]carbamoyl}quinolin-6-yl sulfurofluoridate (**28**)

1-(Fluorosulfuryl)-2,3-dimethyl-1*H*-imidazol-3-ium trifluoromethanesulfonate (SuFEx-IT) (26 mg, 79 µmol, 1.3 eq.) was added to an ice-cold solution of the crude phenol **S8** (22 mg, 61 µmol) and Et_3N (13 µL, 9.3 mg, 92 mmol, 1.5 eq.) in CH_2Cl_2/MeCN (1:3; 4 mL), the cooling bath was removed and the reaction mixture was stirred for 1.5 h. Additional Et_3N (4 µL, 3 mg, 0.5 eq.) and SuFEx-IT (10 mg, 31 µmol, 0.5 eq.) were then added and stirring was continued for another 30 min. Thereafter, a saturated aqueous solution of NH_4Cl (2 mL) was added, the mixture was extracted with CH_2Cl_2 (5×5 mL), and the combined organic fractions were dried and concentrated under reduced pressure. The residue was purified by column chromatography (EtOAc, R_f = 0.32) to yield the raw product **28** (23 mg, 52 µmol) as a yellow oil. Further purification of raw **28** (20 mg) by semi-preparative HPLC (Column: Synergi™ Hydro RP-18e, 80 Å, 4 µm, 21.20×250 mm (Phenomenex, Aschaffenburg, Germany); eluent: 25% MeCN, flow rate: 7.4 mL/min, t_R = 5.8 min) afforded the pure title compound (12%, 3.2 mg, 7.2 µmol; >96% pure) as a colorless solid. **Molecular formula and mass**: $C_{17}H_{13}F_3N_4O_5S$ (442.0559 g/mol). **^{1}H-NMR** [400 MHz, $CDCl_3$, product purified by semi-prep. HPLC]: δ [ppm] = 9.07 (d, *J* = 4.3 Hz, 1 H), 8.53 (d, *J* = 2.5 Hz, 1 H), 8.28 (d, *J* = 9.3 Hz, 1 H), 7.85 (dd, *J* = 9.3, 2.2 Hz, 1 H), 7.71 (d, *J* = 4.3 Hz, 1 H), 7.51 (s_b, 1 H), 5.02 (dd, *J* = 9.0, 3.2 Hz, 1 H), 4.48–3.92 (m, 4 H), 2.90–2.72 (m, 2 H). **^{13}C-NMR** [101 MHz, $CDCl_3$, product purified by column-chrom.]: δ [ppm] = 167.6, 166.5, 151.3, 148.5, 147.6, 140.2, 133.1, 125.2 (t, *J* = 252 Hz), 124.9, 123.4, 120.1, 117.5, 116.2, 52.2 (t, *J* = 32 Hz), 44.5, 42.4, 37.4 (t, *J* = 26 Hz). **^{19}F-NMR** [376 MHz, $CDCl_3$]: δ [ppm] = 37.50 (s, 1 F), -95.80 – -97.58 (m, 1 F), 104.79 – -107.83 (m, 1 F). **HRMS-ESI**: m/z $[M+H]^+$ calculated for $[C_{17}H_{14}F_3N_4O_5S]^+$ = 443.06315, found 443.06288, m/z

[M+Na]$^+$ calculated for [$C_{17}H_{13}F_3N_4O_5SNa$]$^+$ = 465.04510, found: 465.04484. ***R*$_f$ value**: R_f = 0.26 (EtOAc).

4.8.16. Synthesis of 4-{3-[2-(diethylamino)-2-oxoethyl]-5,7-dimethylpyrazolo[1,5-a]pyrimidin-2-yl}phenyl sulfurofluoridate (FS-DPA, **29**)

O-Desmethyl DPA-713 (**S1**) (300 mg, 851 µmol) was dissolved in anhydrous CH_2Cl_2 (50 mL) under heating. Next, Et_3N (189 µL, 138 mg, 1.36 mmol, 1.6 eq.) and SuFEx-IT [33] (363 mg, 1.11 mmol, 1.3 eq.) were added, the mixture was stirred for 2 h and then washed with H_2O (2×40 mL) and brine (40 mL). After drying and concentration under reduced pressure, the residue was purified by column chromatography ($CHCl_3$/acetone = 8:1, R_f = 0.30) to afford the desired product as a colorless solid (296 mg, 80%). **Molecular formula and mass**: $C_{20}H_{23}FN_4O_4S$ (434.349 g/mol). **^{1}H-NMR** [400 MHz, $CDCl_3$]: δ [ppm] = 8.04 (d, *J* = 8.9 Hz, 2H), 7.42 (d, *J* = 8.1 Hz, 2H), 6.56 (s, 1H), 3.93 (s, 2H), 3.56 (q, *J* = 7.1 Hz, 2H), 3.40 (q, *J* = 7.1 Hz, 2H), 2.74 (s, 3H), 2.55 (s, 3H), 1.25 (t, *J* = 7.1 Hz, 4H), 1.10 (t, *J* = 7.1 Hz, 3H). **^{13}C-NMR** [101 MHz, $CDCl_3$]: δ [ppm] = 170.0, 158.1, 153.5, 150.1, 147.7, 145.1, 134.8, 130.9, 121.1, 109.0, 101.8, 42.6, 40.9, 27.9, 24.8, 17.0, 14.6, 13.2. **^{19}F-NMR** [376 MHz, $CDCl_3$]: δ [ppm] = 37.66 (s, 1F). **HRMS-ESI:** m/z [M+H]$^+$ calculated for [$C_{20}H_{24}FN_4O_4S$]$^+$ = 435.14968, found 435.14983, [M+Na]$^+$ calculated for [$C_{20}H_{23}FN_4O_4SNa$]$^+$ = 457.13163, found: 457.13162. ***R*$_f$ value**: R_f = 0.30 ($CHCl_3$/acetone = 8:1).

4.9. Radiochemistry

[^{18}F]Fluoride was produced by the ^{18}O(p,n)^{18}F reaction by bombardment of enriched [^{18}O]water with 17 MeV protons at the BC1710 cyclotron (The Japan Steel Works, Tokyo, Japan) or at a GE PETtrace (GE Healthcare, Chicago, USA) both of the INM-5 (Forschungszentrum Jülich). Radioactivity was measured using a CRC-55tR Dose Calibrator from Capintec, Inc. (Florham Park, Netherlands) and/or a Curiementor 2 (PTW, Freiburg, Germany). The following cartridges were used for radiosyntheses and solid phase extractions (SPE): Sep-Pak Plus C_{18} cartridges (130 mg sorbent, Part No WAT023501, pre-conditioned with 10 mL EtOH and 30 mL H_2O), Sep-Pak® Plus Light QMA Carbonate Cartridge (46 mg Sorbent per Cartridge, 40 µm, not preconditioned) from Waters GmbH (Eschborn, Germany) and Strata™-X 33 µm Polymeric RP cartridges (30 mg sorbent, Part No 8B-S100-TAK; preconditioned with 3 mL EtOH and 10 mL H_2O) from Phenomenex (Aschaffenburg, Germany).

If needed, the identity of radiolabeled products was confirmed by co-injection of the non-radioactive reference compounds, but in most cases the amount of unlabeled precursor was sufficient to be reliably detected and used for identification (the chemical properties of SuFEx-precursors are identical to those of the respective radiolabeled products due to the radiolabeling reaction being an iso-

topic exchange). Radiochemical yields (RCY) corrected for decay to the start of synthesis and/or activity yields (AY) are provided for analytically pure radiolabeled compounds purified by SPE ([^{18}F]**26**–**29**). Radiochemical conversions (RCC) were determined by HPLC analysis after dilution of the reaction mixtures with H_2O. Radioactivity adsorbed to the reactor walls (generally ≤5%) was determined by comparison of the total activity in the reaction vessel before and after complete removal of the reaction mixture. RCCs were determined directly by comparing the peak areas for [^{18}F]fluoride and the radiofluorinated products. For further verification, the decay corrected product peak areas in the chromatograms were compared to the peak area obtained by an injection bypassing the column (corresponds to total activity in the sample volume).

All radiosyntheses were carried out manually according to the radiation protection rules of our institute using appropriate personal protective equipment and shielding. Unless noted otherwise, 5 mL screw top V-Vials® (20-400 thread, 20 mm × 65 mm) were used for all radiosyntheses. Prior to their first use and following every 10–15 reactions, the vials were (re)siliconized to minimize adsorption of [^{18}F]F^- to the vessel walls. To this end, a thin layer of silicone oil (Sigma Aldrich) was applied to the inner surface of the V-Vials®, which were then heated at 310 °C for 12 min and slowly cooled to ambient temperature. That followed, the vials were rinsed (in this order) with EtOAc, CH_2Cl_2, acetone, H_2O, acetone and hot MeOH, after which they were dried at 90 °C for 10 min.

4.9.1. Preparation of [^{18}F]FO_2SO-Ar from FO_2SO-Ar – general procedure 2 (**GP2**)

A precursor stock solution (PSS) was prepared by dissolving the respective aryl fluorosulfate (1.00 mg) in the corresponding solvent (1 mL). An aliquot of this solution was further diluted to the desired concentration (e.g., 200 µL PSS was diluted to a total volume of 10 mL to afford a stock solution with 20 µg/mL precursor). While preparing the dilution series, total pipetting errors were in the range of 2–7%. General protocol: 1. Load [^{18}F]fluoride (approx. 10–30 MBq in 1.0–1.5 mL H_2O) onto a Sep-Pak Accell Plus QMA carbonate cartridge (130 mg sorbent) from the male side. 2. Wash the cartridge with MeOH (2 mL) from the male side. 3. Dry the cartridge with air (20 mL syringe) from the female side, measure activity on the QMA-cartridge. 4. Elute [^{18}F]fluoride with a solution of the corresponding salt (10 mM or 1.5 mM) in MeOH (1 mL or 0.6 mL, resp.) from the female side into the reactor (V-Vial), measure residual activity left on the QMA resin. 5. Evaporate MeOH under reduced pressure in a stream of Ar (approx. 400 mbar) for 3–7 min at 70–90 °C (complete removal of MeOH is essential for the success of radiolabeling!) followed by another 1–2 min at 10 mbar; briefly cool the reactor in a stream of Ar. 6. Add a solution of the corresponding aryl fluorosulfate (0.5–100 nmol, approx. 0.1–20 µg) in the appropriate solvent, typically MeCN (1 mL), and incubate the reaction mixture at 40 °C for 3–7 min without stirring; in the case of the electron deficient substrates, the reaction time should be reduced to 15–45 s in order to avoid decomposition! 7. Add H_2O (≥0.5 mL), shake the resulting mix-

ture vigorously for 30 s and determine the RCC using radio-HPLC or -TLC. For workup and isolation of the radiolabeled product, proceed to step 8. Otherwise, transfer the reaction solution to another vial/waste and determine residual activity left on the reactor walls. Work-up: 8. Dilute the reaction mixture with H_2O (10 mL) and load the crude product onto an appropriate RP-cartridge from the female side, determine activity left in the reactor. 9. Wash the cartridge with H_2O (10 mL) from the female side. 10. Dry the cartridge with air or Ar (50–100 mL). 11. Slowly (>30 s) elute the product with a water-miscible solvent (e.g., EtOH, DMSO, acetone, etc.; ≥0.6 mL). In the case of biocompatible solvents (EtOH or DMSO) dilute with saline to ≤10% (for EtOH) or ≤4% (for DMSO), respectively. Evaporate other organic solvents at 60 °C for 5–10 min and take up the residue in saline or 0.3–1.0% Tween 80 in saline.

4.10. In vivo experiments

All experiments were carried out in accordance with the EU directive 2010/63/EU for animal experiments and the German Animal Welfare Act (TierSchG, 2006) and were approved by the regional authorities (State Office for Nature, Environment and Consumer Protection of North-Rhine Westphalia [LANUV NRW], Dept. Animal Welfare).

4.10.1. Experiments with Boc-Tyr([^{18}F]SO_2F)-OMe ([^{18}F]**26**) in healthy mice (animal license number: 84-02.04.2017.A288.)

Four healthy male C57BL/6 mice (35–40 g) were anesthetized with isoflurane (5% for induction, 2% for maintenance) in O_2/air (3:7), and a catheter for tracer injection was inserted into the lateral tail vein. Mice were placed on an animal holder (Medres, Köln, Germany) and fixed with a tooth bar in a respiratory mask. Body temperature was maintained at 37 °C by continuous warm water flow through the wall of the animal bed. Eyes were protected from drying with Bepanthen eye and nose ointment (Bayer, Leverkusen, Germany). A dynamic PET scan in list mode was conducted using a Focus 220 micro PET scanner (CTI-Siemens, Erlangen, Germany) with a resolution at the center of field of view of 1.4 mm. Data acquisition started with intravenous injection of Boc-Tyr([^{18}F]SO_2F)-OMe (9–11 MBq in 125 µL) and ended after 120 min. This was followed by a 10 min transmission scan using a ^{57}Co point source for attenuation correction. After the scan was finished, the catheter was removed and the mice were allowed to recover in their home cage. After Fourier rebinning, data were reconstructed in two ways: 4 × 30 min frames for visual display and 28 frames (2 × 1 min, 2 × 2 min, 6 × 4 min, 18 × 5 min) for time-activity curves. An iterative OSEM3D/MAP algorithm with attenuation and decay correction was used. The resulting voxel sizes were 0.47 mm x 0.47 mm x 0.80 mm. All further analysis was performed with the software VINCI 4.72 (Max Planck Institute for Metabolism Research, Cologne, Germany). Standardized uptake values based on body weight (SUV_{bw}) were de-

termined according to the following equation: SUV_{bw}= radioactivity [Bq/g] × body weight [g] × 100 / injected dose [Bq]

4.10.2. Experiments with H-Tyr([^{18}F]SO_2F)-OMe ([^{18}F]**27**) in rats bearing orthotopic U87 MG gliomas (animal license number: 84-02.04.2017.A288)

U87 MG glioma cells (10^5 cells in 1 µL) were implanted stereotactically under inhalation anesthesia (initial dosage of 5% isoflurane in O_2/air (3:7), maintenance 3–4% isoflurane) into the brain of two immunodeficient male Rowett Nude Rats (Charles River, Sulzfeld, Germany) weighting 268–321 g. The stereotactic coordinates were 0.5 mm anterior, 2.5 mm lateral and 3 mm ventral from Bregma. MRI scans were performed one, two and three weeks after tumor cell implantation to determine the size of the intracranial tumors. The measurements were performed under general anesthesia (initial dosage of 5% isoflurane in O_2/air (3:7), maintenance 2–2.5% isoflurane) in an MRI scanner (3T Achieva®, Philips Healthcare, Best, The Netherlands) in combination with an 8 Channel Volumetric Rat Array (Rapid Biomedical GmbH, Rimpar, Germany). Three dimensional T2-weighted MR images were acquired using a turbo-spin echo sequence with repetition time = 14 s, echo time = 30 ms, field of view = 60 × 60 × 60 mm^3 and voxel size = 0.5 × 0.5 × 0.5 mm^3. H-Tyr([^{18}F]SO_2F)-OMe-PET measurements took place 23 days after tumor implantation as described above, with i.v. application of 64–66 MBq tracer in 500 µL. Emission data was collected for 60 min, followed by a transmission scan.

4.10.3. Experiments with [^{18}F]FS-UAMC1110 ([^{18}F]**28**) in mice bearing subcutaneous HT1080 or HT1080-FAP tumors (animal license number: 81-02.04.2020.A348)

To deactivate natural killer cells, 100 µL of anti-Asialo (0.2 mg/mL 0.9 % NaCl; Fujifilm Wako Chemicals Europe, Neuss, Germany) were injected intraperitoneally 24 h prior to tumor implantation in four CB17-SCID mice (Janvier, Le-Genest-Saint-Isle, France) weighting 17–22 g. The following day, two CB17-SCID mice (one male and one female) were subcutaneously implanted with 2×10^6 HT1080 fibrosarcoma cells transfected with the human FAP gene (HT1080-FAP, kindly provided by Uwe Haberkorn, University Hospital Heidelberg, Germany) in 80 µL Corning Matrigel (Merck, Darmstadt, Germany) at the right shoulder. Two additional CB17-SCID mice (one male and one female) were implanted with 2×10^6 wildtype HT1080 cells (DMSZ, Braunschweig, Germany). After two weeks of tumor growth, the four mice were measured with [^{18}F]FS-UAMC1110 (9–10 MBq in 125 µL) as described above.

4.10.4. Experiments with [^{18}F]FS-DPA ([^{18}F]**29**) in a neuroinflammation rat model (animal license number: 84-02.04.2017.A288)

Endothelin-1 (stabilized; 300 pmol in 1.5 µL NaCl; Merck, Darmstadt, Germany) was stereotactically injected at the coordinates 1.5 mm anterior, 0 mm lateral and 3.3 mm ventral from Bregma to induce transient occlusion of the anterior cerebral artery (ACAo) followed by persistent neuroinflammation in three male Sprague Dawley rats (Janvier, Le-Genest-Saint-Isle, France) weighting 758–862 g. MRI was performed after 24 h as described above. Four weeks after ACAo, rats were measured with [^{18}F]FS-DPA (64–71 MBq in 500 µL) as described above.

5. Supplementary data:

Extended experimental information and analytical data are provided in the supplementary information (SI).

6. Acknowledgements

This work was supported by the DFG grant ZL 65/4-1.

7. Competing interests statement

The authors declare that they have no known competing financial interests or personal relationships that could have appeared to influence the work reported in this paper.

8. References

[1] V. Duclos, A. Iep, L. Gomez, L. Goldfarb, F.L. Besson, PET Molecular Imaging: A Holistic Review of Current Practice and Emerging Perspectives for Diagnosis, Therapeutic Evaluation and Prognosis in Clinical Oncology, Int. J. Mol. Sci. 22 (2021) 4159. https://doi.org/10.3390/ijms22084159.

[2] Z. Brady, M.L. Taylor, M. Haynes, M. Whitaker, A. Mullen, L. Clews, M. Partridge, R.J. Hicks, J. V. Trapp, The clinical application of PET/CT: A contemporary review., Australas. Phys. Eng. Sci. Med. 31 (2008) 90–109. https://doi.org/10.1007/BF03178584.

[3] N.S. Goud, R.K. Joshi, R.D. Bharath, P. Kumar, Fluorine-18: A radionuclide with diverse range of radiochemistry and synthesis strategies for target based PET diagnosis, Eur. J. Med. Chem. 187 (2020) 111979. https://doi.org/10.1016/j.ejmech.2019.111979.

[4] K.R. Scroggie, M. V. Perkins, J.M. Chalker, Reaction of [^{18}F]Fluoride at Heteroatoms and Metals for Imaging of Peptides and Proteins by Positron Emission Tomography, Front. Chem. 9 (2021) 687678. https://doi.org/10.3389/fchem.2021.687678.

[5] Q. Zheng, H. Xu, H. Wang, W.-G.H. Du, N. Wang, H. Xiong, Y. Gu, L. Noodleman, K.B. Sharpless, G. Yang, P. Wu, Sulfur [^{18}F]Fluoride Exchange Click Chemistry Enabled Ultrafast Late-Stage Radiosynthesis, J. Am. Chem. Soc. 143 (2021) 3753–3763. https://doi.org/10.1021/jacs.0c09306.

[6] B.D. Zlatopolskiy, J. Zischler, D. Schäfer, E.A. Urusova, M. Guliyev, O. Bannykh, H. Endepols, B. Neumaier, Discovery of 7-[^{18}F]fluorotryptophan as a novel positron emission tomography (PET) probe for the visualization of tryptophan metabolism in vivo., J. Med. Chem. 61 (2018) 189–206. https://doi.org/10.1021/acs.jmedchem.7b01245.

[7] B.D. Zlatopolskiy, H. Endepols, P. Krapf, M. Guliyev, E.A. Urusova, R. Richarz, M. Hohberg, M. Dietlein, A. Drzezga, B. Neumaier, Discovery of ^{18}F-JK-PSMA-7, a PET probe for the detection of small PSMA-positive lesions., J. Nucl. Med. 60 (2019) 817–823. https://doi.org/10.2967/jnumed.118.218495.

[8] A. Craig, N. Kolks, E.A. Urusova, J. Zischler, M. Brugger, H. Endepols, B. Neumaier, B.D. Zlatopolskiy, Preparation of labeled aromatic amino acids via late-stage ^{18}F-fluorination of chiral nickel and copper complexes., Chem. Commun. 56 (2020) 9505–9508. https://doi.org/10.1039/D0CC02223C.

[9] B.D. Zlatopolskiy, F. Neumaier, T. Rüngeler, B. Drewes, N. Kolks, B. Neumaier, Preparation of a first ^{18}F-labeled agonist for M1 muscarinic acetylcholine receptors., Molecules. 25 (2020) 2880. https://doi.org/10.3390/molecules25122880.

[10] C. Hoffmann, S. Evcüman, F. Neumaier, B.D. Zlatopolskiy, S. Humpert, D. Bier, M. Holschbach, A. Schulze, H. Endepols, B. Neumaier, [^{18}F]ALX5406: A brain-penetrating prodrug for GlyT1-specific PET imaging., ACS Chem. Neurosci. 12 (2021) 3335–3346. https://doi.org/10.1021/acschemneuro.1c00284.

[11] D. Ory, J. Van den Brande, T. de Groot, K. Serdons, M. Bex, L. Declercq, F. Cleeren, M. Ooms, K. Van Laere, A. Verbruggen, G. Bormans, Retention of [^{18}F]fluoride on reversed phase HPLC columns, J. Pharm. Biomed. Anal. 111 (2015) 209–214. https://doi.org/10.1016/j.jpba.2015.04.009.

[12] R. Richarz, P. Krapf, F. Zarrad, E.A. Urusova, B. Neumaier, B.D. Zlatopolskiy, Neither azeotropic drying, nor base nor other additives: A minimalist approach to ^{18}F-labeling., Org. Biomol. Chem. 12 (2014) 8094–8099. https://doi.org/10.1039/C4OB01336K.

[13] F. Zarrad, B.D. Zlatopolskiy, P. Krapf, J. Zischler, B. Neumaier, A practical method for the

preparation of ^{18}F-labeled aromatic amino acids from nucleophilic [^{18}F]fluoride and stannyl precursors for electrophilic radiohalogenation, Molecules. 22 (2017) 2231. https://doi.org/10.3390/molecules22122231.

[14] H.H. Coenen, A.D. Gee, M. Adam, G. Antoni, C.S. Cutler, Y. Fujibayashi, J.M. Jeong, R.H. Mach, T.L. Mindt, V.W. Pike, A.D. Windhorst, Consensus nomenclature rules for radiopharmaceutical chemistry — Setting the record straight, Nucl. Med. Biol. 55 (2017) v–xi. https://doi.org/10.1016/j.nucmedbio.2017.09.004.

[15] D.Y. Lewis, R. Mair, A. Wright, K. Allinson, S.K. Lyons, T. Booth, J. Jones, R. Bielik, D. Soloviev, K.M. Brindle, [^{18}F]fluoroethyltyrosine-induced Cerenkov Luminescence Improves Image-Guided Surgical Resection of Glioma, Theranostics. 8 (2018) 3991–4002. https://doi.org/10.7150/thno.23709.

[16] F. Krämer, B. Gröner, C. Hoffmann, A. Craig, M. Brugger, A. Drzezga, M. Timmer, F. Neumaier, B.D. Zlatopolskiy, H. Endepols, B. Neumaier, Evaluation of 3-L- and 3-D-[^{18}F]Fluorophenylalanines as PET-tracers for Tumor Imaging., Cancers (Basel). 13 (2021) 6030.

[17] K.-J. Langen, G. Stoffels, C. Filss, A. Heinzel, C. Stegmayr, P. Lohmann, A. Willuweit, B. Neumaier, F.M. Mottaghy, N. Galldiks, Imaging of amino acid transport in brain tumours: Positron emission tomography with O-(2-[^{18}F]fluoroethyl)-L-tyrosine (FET)., Methods. 130 (2017) 124–134. https://doi.org/10.1016/j.ymeth.2017.05.019.

[18] L. Xin, J. Gao, Z. Zheng, Y. Chen, S. Lv, Z. Zhao, C. Yu, X. Yang, R. Zhang, Fibroblast Activation Protein-α as a Target in the Bench-to-Bedside Diagnosis and Treatment of Tumors: A Narrative Review, Front. Oncol. 11 (2021) 648187. https://doi.org/10.3389/fonc.2021.648187.

[19] E. Puré, R. Blomberg, Pro-tumorigenic roles of fibroblast activation protein in cancer: back to the basics, Oncogene. 37 (2018) 4343–4357. https://doi.org/10.1038/s41388-018-0275-3.

[20] A. Altmann, U. Haberkorn, J. Siveke, The Latest Developments in Imaging of Fibroblast Activation Protein, J. Nucl. Med. 62 (2021) 160–167. https://doi.org/10.2967/jnumed.120.244806.

[21] S. Imlimthan, E. Moon, H. Rathke, A. Afshar-Oromieh, F. Rösch, A. Rominger, E. Gourni, New Frontiers in Cancer Imaging and Therapy Based on Radiolabeled Fibroblast Activation Protein Inhibitors: A Rational Review and Current Progress, Pharmaceuticals. 14 (2021) 1023. https://doi.org/10.3390/ph14101023.

[22] K. Jansen, L. Heirbaut, R. Verkerk, J.D. Cheng, J. Joossens, P. Cos, L. Maes, A.-M. Lambeir, I. De Meester, K. Augustyns, P. Van der Veken, Extended Structure–Activity Relationship and Pharmacokinetic Investigation of (4-Quinolinoyl)glycyl-2-cyanopyrrolidine Inhibitors of Fibroblast Activation Protein (FAP), J. Med. Chem. 57 (2014) 3053–3074. https://doi.org/10.1021/jm500031w.

[23] B. Zinnhardt, F. Roncaroli, C. Foray, E. Agushi, B. Osrah, G. Hugon, A.H. Jacobs, A. Winkeler, Imaging of the glioma microenvironment by TSPO PET, Eur. J. Nucl. Med. Mol. Imaging. 49 (2021) 174–185. https://doi.org/10.1007/s00259-021-05276-5.

[24] E.L. Werry, F.M. Bright, M. Kassiou, TSPO PET Imaging as a Biomarker of Neuroinflammation in Neurodegenerative Disorders, in: P. V. Peplow, B. Martinez, T.A. Gennarelli (Eds.), Neurodegener. Dis. Biomarkers. Neuromethods, Vol 173, Humana Press, New York, NY, 2022: pp. 407–427. https://doi.org/10.1007/978-1-0716-1712-0_17.

[25] L.J. De Picker, B.C.M. Haarman, Applicability, potential and limitations of TSPO PET imaging as a clinical immunopsychiatry biomarker, Eur. J. Nucl. Med. Mol. Imaging. 49 (2021) 164–173. https://doi.org/10.1007/s00259-021-05308-0.

[26] H. Endepols, H. Mertgens, H. Backes, U. Himmelreich, B. Neumaier, R. Graf, G. Mies, Longitudinal assessment of infarct progression, brain metabolism and behavior following anterior cerebral artery occlusion in rats, J. Neurosci. Methods. 253 (2015) 279–291. https://doi.org/10.1016/j.jneumeth.2014.11.003.

[27] H. Zhou, P. Mukherjee, R. Liu, E. Evrard, D. Wang, J.M. Humphrey, T.W. Butler, L.R. Hoth, J.B. Sperry, S.K. Sakata, C.J. Helal, C.W. am Ende, Introduction of a Crystalline, Shelf-Stable Reagent for the Synthesis of Sulfur(VI) Fluorides, Org. Lett. 20 (2018) 812–815. https://doi.org/10.1021/acs.orglett.7b03950.

[28] M.L. James, R.R. Fulton, D.J. Henderson, S. Eberl, S.R. Meikle, S. Thomson, R.D. Allan, F. Dolle, M.J. Fulham, M. Kassiou, Synthesis and in vivo evaluation of a novel peripheral benzodiazepine receptor PET radioligand, Bioorg. Med. Chem. 13 (2005) 6188–6194. https://doi.org/10.1016/j.bmc.2005.06.030.

[29] S.D. Schimler, M.A. Cismesia, P.S. Hanley, R.D.J. Froese, M.J. Jansma, D.C. Bland, M.S. Sanford, Nucleophilic Deoxyfluorination of Phenols via Aryl Fluorosulfonate Intermediates., J. Am. Chem. Soc. 139 (2017) 1452–1455. https://doi.org/10.1021/jacs.6b12911.

[30] G. Zhou, X. Deng, C. Pan, E.T.L. Goh, R. Lakshminarayanan, R. Srinivasan, SLAP reagents for the

photocatalytic synthesis of C3/C5-substituted, N-unprotected selenomorpholines and 1,4-selenazepanes., Chem. Commun. (Camb). 56 (2020) 12546–12549. https://doi.org/10.1039/d0cc04471g.

[31] C.J. Smedley, J.A. Homer, T.L. Gialelis, A.S. Barrow, R.A. Koelln, J.E. Moses, Accelerated SuFEx Click Chemistry For Modular Synthesis., Angew. Chem. Int. Ed. Engl. 61 (2022) e202112375. https://doi.org/10.1002/anie.202112375.

[32] C. Veryser, J. Demaerel, V. Bieliu Nas, P. Gilles, W.M. De Borggraeve, Ex Situ Generation of Sulfuryl Fluoride for the Synthesis of Aryl Fluorosulfates., Org. Lett. 19 (2017) 5244–5247. https://doi.org/10.1021/acs.orglett.7b02522.

[33] T. Guo, G. Meng, X. Zhan, Q. Yang, T. Ma, L. Xu, K.B. Sharpless, J. Dong, A New Portal to SuFEx Click Chemistry: A Stable Fluorosulfuryl Imidazolium Salt Emerging as an "F−SO_2+" Donor of Unprecedented Reactivity, Selectivity, and Scope, Angew. Chemie Int. Ed. 57 (2018) 2605–2610. https://doi.org/10.1002/anie.201712429.